Innovations Deserving
Exploratory Analysis Programs

NCHRP IDEA Program

Contactless Electrode for Fast Survey of Concrete Reinforcement Corrosion

Final Report for
NCHRP IDEA Project 176

Prepared by:
Alberto A. Sagüés and Leonidas Emmenegger
University of Florida

January 2017

TRANSPORTATION RESEARCH BOARD
The National Academies of
SCIENCES · ENGINEERING · MEDICINE

Innovations Deserving Exploratory Analysis (IDEA) Programs Managed by the Transportation Research Board

This IDEA project was funded by the NCHRP IDEA Program.

The TRB currently manages the following three IDEA programs:

- The NCHRP IDEA Program, which focuses on advances in the design, construction, and maintenance of highway systems, is funded by American Association of State Highway and Transportation Officials (AASHTO) as part of the National Cooperative Highway Research Program (NCHRP).
- The Safety IDEA Program currently focuses on innovative approaches for improving railroad safety or performance. The program is currently funded by the Federal Railroad Administration (FRA). The program was previously jointly funded by the Federal Motor Carrier Safety Administration (FMCSA) and the FRA.
- The Transit IDEA Program, which supports development and testing of innovative concepts and methods for advancing transit practice, is funded by the Federal Transit Administration (FTA) as part of the Transit Cooperative Research Program (TCRP).

Management of the three IDEA programs is coordinated to promote the development and testing of innovative concepts, methods, and technologies.

For information on the IDEA programs, check the IDEA website (www.trb.org/idea). For questions, contact the IDEA programs office by telephone at (202) 334-3310.

IDEA Programs
Transportation Research Board
500 Fifth Street, NW
Washington, DC 20001

Contactless Electrode for Fast Survey of Concrete Reinforcement Corrosion

IDEA Program Final Report

NCHRP IDEA Project 176

Prepared for the NCHRP IDEA Program

Transportation Research Board

National Research Council

Prepared by Alberto A. Sagüés (Principal Investigator) and Leonidas Emmenegger

Department of Civil and Environmental Engineering

University of South Florida

Tampa, Florida 33620

January 26, 2017

ACKNOWLEDGMENTS

The authors thank Dr. Inam Jawed of NCHRP and the members of the Expert Review Panel for their valuable input in steering this project:

Chair: Mario Paredes—TRI
Members:
Michael Brown—Virginia DOT/(Michael Sprinkel VDOT)
Raymond Bottenberg—Oregon DOT
Hamid Ghasemi—FHWA
Ivan Lasa—Florida DOT
S.-K. Lee—SK Lee and Associates
Ali Sohanghpurwala—Concorr Inc.
Siva Venugopalan—SCS Inc.
Y. Paul Virmani—FHWA

The extensive dedication and valuable contribution of Mr. Jordan Riber-Smith in processing of the field data, including implementation of deconvolution algorithms, is gratefully acknowledged. The authors are indebted to Mr. Hani Freij and Connor Fries of USF for their assistance in performing the field tests and in particular to David Dukeman for participation in the tests and improving the test equipment. Special thanks are given to the members of the Florida DOT Materials Office Corrosion group for their cooperation and assistance in preparing the site at the Sunshine Skyway fishing pier for the field tests. Helpful discussions with Dr. Sylvia Kessler on the processing and interpretation of the field tests were much appreciated. The assistance of Dr. M. Celestine in creating a distance transducer for position recording is gratefully acknowledged.

TABLE OF CONTENTS

1. EXECUTIVE SUMMARY

Corrosion of steel reinforcement from deicing salts or marine exposure severely limits the service life of reinforced concrete highway bridges in the United States. Early detection of corrosion is particularly desirable, especially if testing can be performed rapidly and with little disruption of the structure or traffic. Electric potential mapping of the concrete surface, using reference ("half-cell") electrodes temporarily placed on the surface, is the most common form of nondestructive electrochemical corrosion assessment in reinforced concrete. The method is used by many state transportation agencies, and the methodology is standardized by ASTM. The detection is based on the drop in steel potential that takes place on corrosion initiation, to a value hundreds of mV more negative than before. A map of potential as function of surface position can thus identify the location and size of the corroding regions.

While useful, present potential mapping methods require appreciable time for execution, which can be an important factor in dissuading otherwise frequent evaluations, especially for highway bridge decks where lane closures are very disruptive. The most important obstacle to very rapid mapping is stabilization delays stemming from the use, until now, of conventional reference electrodes that must be placed in physical contact with the concrete surface. Exchange of electrolytes at the contact point requires stabilization time, which delays the measurements, an important factor when hundreds of measurements are often required.

This project developed an alternative, fast responding, noncontacting electrode that requires no surface pretreatment and avoids much of the delays and disruption associated with conventional reference electrodes. The sensor is conceptually suitable for operation from moving vehicles, offering the opportunity for extensive corrosion assessment that would be prohibitively expensive at present. The technology can become a powerful additional tool for rapid assessment of corrosion condition of bridges at low cost, permitting much wider deployment than present methods, and improving the ability of transportation agencies to implement timely corrosion control measures. This novel electrode sensor is based on the Kelvin Probe (KP hereafter) principle, which had been recently adapted to concrete surfaces with highly encouraging results. The electrode does not require physical contact with the surface; therefore, no surface preparation or electrolyte stabilization is required. Thus, bridge deck surface potential maps can be obtained from a moving platform and in a time frame much faster than that obtained with the conventional method.

The project expanded the small scale device used in a previous investigation and demonstrated its application on an actual bridge deck environment. The following summarizes the main accomplishments.

An initial conceptual KP for a contactless steel potential survey of reinforced concrete was scaled up dimensionally in both disk diameter (to 10 cm), disk-to-concrete surface operating gap (to as much as ~2 cm), and in an electromagnetic driving unit (to a commercially available vibrator operation) in a rugged configuration suitable for an actual road surface. Laboratory tests with the scaled-up probe showed that corrections for operating gap changes may be conducted by appropriate calibration. Hence, precise real-time gap control beyond that achievable by appropriately selected wheel base dimensions was not found to be necessary.

Test runs conducted with a single probe prototype on laboratory concrete specimens and on an outdoor large-size slab demonstrated the ability to acquire potential maps. The contactless probe potential maps on the outdoor slab successfully identified the anodic spot on the slab and provided information in

excellent graphic agreement with results obtained by conventional half-cell electrode surveys. The tests also illustrated how calibration for absolute potential measurements can be conducted. Analysis of single probe operation parameters for measurements in moving vehicles was conducted, indicating good potential for readings at practical speeds. An even faster alternative mode was proposed for future examination.

The single KP was duplicated and the two units integrated as a dual KP array capable of synchronized operation. The dual probe array was integrated on a robust wheeled platform. The dual KP array includes digital signal processing and control operating from an onboard laptop computer and off-the-shelf data acquisition boards, active shields that provide compensation for operating gap variations, and adjustments for optimizing probe response speed with system stability. A specialized data deconvolution procedure was developed and successfully deployed to allow for better interpretation of results obtained with the probe array in motion.

Probe array operation was demonstrated by two field test series conducted at a bridge deck exposed to marine service conditions, part of the former west access road of the old Florida Sunshine Skyway Bridge in Tampa Bay. Both tests series included operation of the dual KP array with operating gaps of 1 cm and 2 cm. The results were compared with those from a potential survey of the same deck portion using a conventional copper/copper sulfate electrode (CSE).

The field tests provided, as the main outcome of the project, a demonstration of the practical feasibility of the concept of using a rapidly scanning contactless surface probe to conduct potential mapping of a highway bridge surface for corrosion detection. The contactless KP maps successfully replicated the features obtained with the CSE mapping procedure, but at a much faster rate and without need to prepare the surface or waiting time for stabilization. The field tests also demonstrated the practical feasibility of multiple probes operating together and in synchronized fashion to scan simultaneously parallel portions of a lane in a bridge deck. Results of exploratory tests suggested that deck surface conditions including painted lane dividers, wetting, and motor oil spots do not severely affect the readings by the dual KP array.

The signal processing methodology developed here could be easily expanded, with ordinary consumer's electronics, to a multiple sensor array sufficient in size to cover the width of an entire traffic lane. Probe array operation was best when operating at a 1-cm, disk-bridge deck distance gap. Operation at a 2-cm gap still provided useful results; however, increasing scatter indicated that 2 cm is near the upper limit of practical operation at the present state of development. Larger operating gaps are expected to be feasible however given subsequent development.

Availability of contactless probe systems could dramatically expand the development and updating of corrosion condition information on much of the national bridge deck inventory in deicing salt and marine regimes. Operations that in the past required extended lane closures and costly labor contracts could now be conducted with minimal traffic disruption and at fraction of the cost.

Planning for implementation of the product included contacting future potential partners as well as agencies engaged in bridge performance and robotic assessment methods for bridge deck assessment. A U.S. Patent application on this methodology has been filed by the University of South Florida. Work in progress in this project was disseminated at various technical venues.

2. THE PRODUCT

This project developed and demonstrated a Kelvin Probe (KP) device that samples the surface of reinforced concrete with a novel contactless electrode, providing rapid and stable electrode potential mapping for early corrosion detection in highway structures.

Corrosion of steel reinforcement from deicing salts or marine exposure severely limits the service life of reinforced concrete highway bridges in the United States. Early detection of corrosion is particularly desirable, especially if testing can be performed rapidly and with little disruption of the structure or traffic. Electric potential mapping of the concrete surface, using reference ("half-cell") electrodes temporarily placed on the surface, is the most common form of nondestructive electrochemical corrosion assessment in reinforced concrete, identifying the locations on a bridge deck surface beneath which corrosion of reinforcement is in progress. However, conventional methods for mapping use wet tip, regular reference electrodes that are slow to respond and that require surface preparation. Thus, present potential mapping methods require appreciable time for execution, which can be an important factor in dissuading otherwise frequent evaluations, especially for highway bridge decks where lane closures are very disruptive.

The novel electrode sensor developed here is based on the KP principle, which had been recently adapted to concrete surfaces with highly encouraging results. The electrode does not require physical contact with the surface so no surface preparation or electrolyte stabilization is required. Therefore, bridge deck surface potential maps can be obtained from a moving platform and in a time frame much faster than that obtained with the conventional method. This project expanded the small scale device used in a previous investigation and demonstrated its application on an actual bridge deck environment.

The project scaled up earlier small laboratory units into a robust, dual array system capable of operating on an actual bridge deck surface. Probe array operation was demonstrated by two field test series conducted at a bridge deck exposed to marine service conditions, part of the former west access road of the old Sunshine Skyway Bridge in Tampa Bay. The contactless KP maps successfully replicated the features obtained with the conventional contact electrode mapping procedure, but at a much faster rate and without need to prepare the surface or wait for stabilization. The field tests also demonstrated the practical feasibility of multiple probes operating together and in synchronized fashion to scan parallel portions of a lane in a bridge deck simultaneously.

The signal processing methodology developed here could be easily expanded, with ordinary consumer's electronics, to a multiple sensor array sufficient in size to cover the width of an entire traffic lane. Availability of contactless probe systems could dramatically expand the development and updating of corrosion condition information on much of the national bridge deck inventory in deicing salt and marine regimes. Operations that in the past required extended lane closures and costly labor contracts could now be conducted with minimal traffic disruption and at fractional cost.

Planning for implementation of the product included contacting future potential partners as well as agencies engaged in bridge performance and robotic assessment methods for bridge deck assessment. A U.S. Patent application on this methodology has been filed by the University of South Florida. Work in progress in this project was disseminated at various technical venues.

3. CONCEPT AND INNOVATION

Present Technology and a Limit for Wider Deployment

Corrosion of steel reinforcement from deicing salts or marine exposure severely limits the service life of reinforced concrete highway bridges in the United States [*1,2*]. Early detection of corrosion is particularly desirable, especially if testing can be performed rapidly and with little disruption of the structure or traffic. Potential mapping is the most common form of nondestructive electrochemical corrosion assessment in reinforced concrete. The technique uses reference ("half-cell") electrodes temporarily placed on the concrete surface [*3–6*]. It is particularly suited for plain rebar bridge decks in deicing salt regimes and it is used by many state transportation agencies [*3*]. Methodology is standardized in ASTM C-876 09 [*4*]. The method is based on the drop in steel potential that takes place on corrosion initiation, to a value hundreds of mV more negative than before. A map of potential as function of surface position can identify the location and size of the corroding regions. Useful results are obtained even if only relative potential measurements are available, since the corrosion location is still indicated by the potential gradient between points of the concrete surface.

While useful, present potential mapping methods require appreciable time for execution, which can be an important factor in dissuading otherwise frequent evaluations, especially for highway bridge decks where lane closures are very disruptive. Some delay is involved in making the needed metallic contact to the rebar assembly; however, that is a one-time task that can be performed earlier by an advance crew. The most important obstacle to very rapid testing is stabilization delays stemming from the use, until now, of conventional reference electrodes. Those are usually of the $Cu/CuSO_4$ (CSE) type and are normally fitted with a soft electrolytic intermediary such as a moist sponge that must be placed in physical contact with the concrete surface.

The need to wait for stabilization of the measured potential value occurs because the electrode requires an electrolytic path from the pore water in concrete to the electrolyte in the sponge, and then to the internal electrolyte of the electrode. The path is completed when the sponge contacts the concrete surface. Since the latter is normally not saturated with water, electrolyte from the sponge flows by suction into the concrete pores. This flow disrupts the electrolytic configuration of the pore water and can introduce substantial drift in the potential reading (e.g., by > 150 mV) over a time scale of minutes or hours, but with an appreciable fraction taking place during the first few seconds following contact [*7–9*]. The extent and time scale of the phenomenon may vary depending on surface condition so it cannot be easily compensated. Considerable scatter in the measurements may therefore ensue from measurement instability, with corresponding uncertainty in the location of the corroding zone. The instability is partially solved by topical pre-wetting of the surface followed by a conditioning delay, but at the cost of added test time and the consequences noted above. Additional uncertainty may result in instances (e.g., during a dry period) when surface wetting could substantially increase the coupling between anodic and cathodic regions. In such event, the overall corrosion condition of the system itself would be disturbed and the measured corrosion pattern could be misleading.

Potential surveys on a typical bridge deck involve conducting numerous measurements [*4–6*]. The delays and uncertainties discussed above place a large cumulative demand on test time and labor costs, further compounded if lengthy lane closures are needed. Comparable issues would be present even if continuous potential recording devices using moist rolling contacts were used [*10*], because surface conditioning delays

would still exist. Those factors inhibit frequent deployment of potential surveys with consequent lesser opportunity for early corrosion detection and resulting maintenance management measures. A novel testing approach to remove this limitation is presented next.

Novel Non-contacting Kelvin Probe Electrode for Concrete

This project developed an alternative, fast responding, non-contacting electrode that requires no surface pretreatment, and avoids much of the delays and disruptions associated with conventional reference electrodes. The sensor is conceptually suitable for operation from moving vehicles, offering the opportunity for extensive corrosion assessment that would be prohibitively expensive at present. The technology can become a powerful additional tool for rapid assessment of corrosion condition of bridges at low cost, permitting much wider deployment than present methods, and improving the ability of transportation agencies to implement timely corrosion control measures.

This novel electrode sensor is based on the KP principle and was recently introduced by the proposer [*11*] with highly encouraging results. The KP has long been used in other science and engineering fields [*12–14*], but until recently unexplored for concrete applications, for which it represents a radical innovation. The surface potential is measured, without physical contact, by a metallic reference plate that oscillates near the concrete surface acting as a variable capacitor. Except for a master contact to one point of the continuous rebar assembly (which may be obviated in Differential mode as described later) the probe is non-intrusive, as no wetting or contact with the concrete surface is needed. The probe provides nearly instantaneous and drift-free potential readings even for long-term dried concrete surfaces [*11*].

A detailed description of the factors relevant to application of the KP to concrete is given elsewhere [*11*] so only a brief summary is presented here. The KP determines the potential difference E between two surfaces facing each other and designated as working and reference, respectively. In the present case the working surface is a small part of the outer concrete surface, and the reference surface is one side of a small disk of stainless steel or other suitable alloy. The disk and the concrete surfaces are separated by a small distance h forming a parallel-plate capacitor configuration. The disk is connected through electronic conductors to the rebar assembly in the concrete. Consequently, the concrete and the reference surfaces are joined through an electronic and electrolytic conductive path with associated interfaces that determine the value of E, which is equal to the steel potential plus a constant for a given concrete surface condition and disk material [*11*].

In the KP the distance h is rapidly varied by attaching the disk to an insulating, vertically vibrating stem. Consequently, the charge on the capacitor changes as well, causing an alternating current to circulate through the conductive path. The value of E is then determined by a zeroing process whereby a source of known potential but of opposite polarity to E is inserted in the circuit path and varied until the alternating current vanishes. That condition is obtained when the inserted source potential is numerically equal to E, hence providing its value. The zeroing is performed automatically with ordinary control circuitry, yielding an immediate record of the value of E. Hovering the probe over different places on the concrete surface then yields E values that can be used to build a potential map suitable for identification of corroding spots, but without any need for physical contact or disturbance of the concrete surface. Importantly, the result is not highly sensitive to the exact value of h, so vertical positioning is not critical. A non-vibrating operating mode

is also possible for the KP, allowing for fast travel speeds; however, in that case gap control is more exacting [*14*].

Promising Initial Trials

A laboratory trial prototype of the probe was successfully created in recent work by the proposer, as shown in Figure 1 [*11*]. The probe had a 1.3-cm-diameter stainless steel reference disk vibrating at ~150 Hz with amplitude h_A = 0.5 mm, actuated with a voice coil electromagnetic driver. At rest the gap distance was h = 1 mm. A metal casing provided shielding. Insulated stop screws around the skirt perimeter ensured stable positioning against flat surfaces. Zeroing was made automatically with a feedback circuit, and the value of E was acquired digitally. Custom circuitry used ordinary off-the-shelf components.

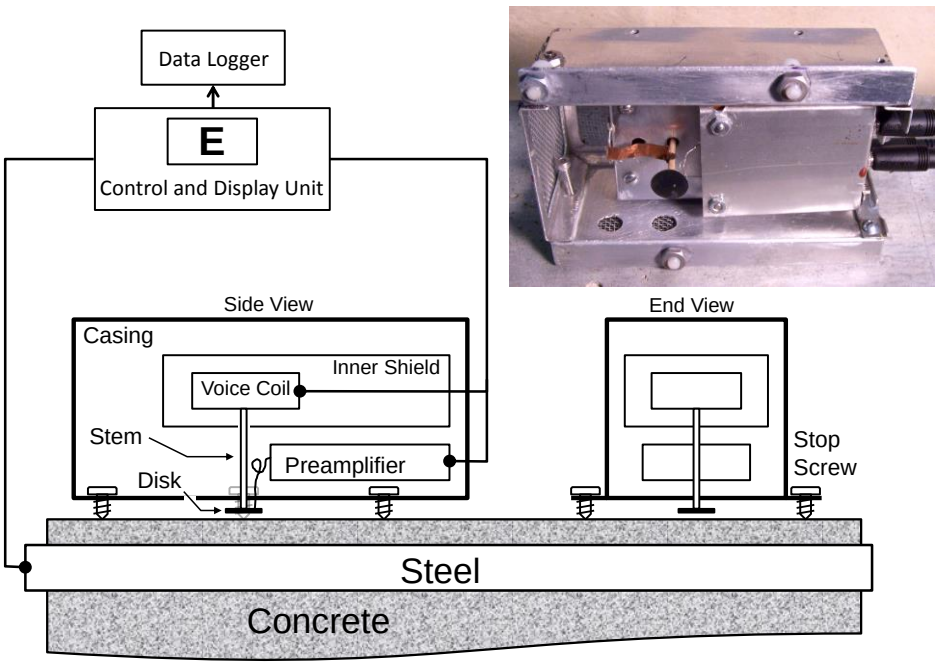

Figure 1: Trial KP prototype. Full details are provided in Sagüés and Walsh [*11*] from which this figure was adapted.

Performance of the probe prototype was highly encouraging. Findings are fully detailed in Sagüés and Walsh [*11*] and included the following:

<u>Rapid response, high stability:</u> When placed on a stable concrete surface the KP provided nearly instantaneous and far more stable readings than those of a conventional wet-tip reference electrode. This is shown in Figure 2, which also reveals much greater drift of the potential measured with a conventional electrode (using a wet sponge tip as is customary) when placing the electrode without pre-wetting the surface on the same point evaluated earlier by the KP. As noted earlier, that drift reflects electrolytic rearrangement in the pore network of the concrete near the surface as it is penetrated by the water from the sponge, with consequent slow establishment of a new diffusion potential regime. No such disturbance takes place with the contactless KP. The nearly instant stabilization of the KP output compared with the drift affecting the

conventional electrode is the key factor in the ability of the KP to deliver rapid assessment of corrosion potentials and its application to a fast survey system. Tolerance to changes in the vertical placement *h* of the probe was good as well, as expected from the operating principle of the KP. Increasing *h* by 100% in a given test spot resulted in potential reading shifts of less than 40 mV. It is noted that in a typical half-cell field survey using a conventional electrode, a potential drift condition of the extent noted in Figure 2 would require pre-wetting of the surface and verification of stable readings afterwards, with consequent operational delays and/or uncertainty as to whether stability has been reached on the entire test surface.

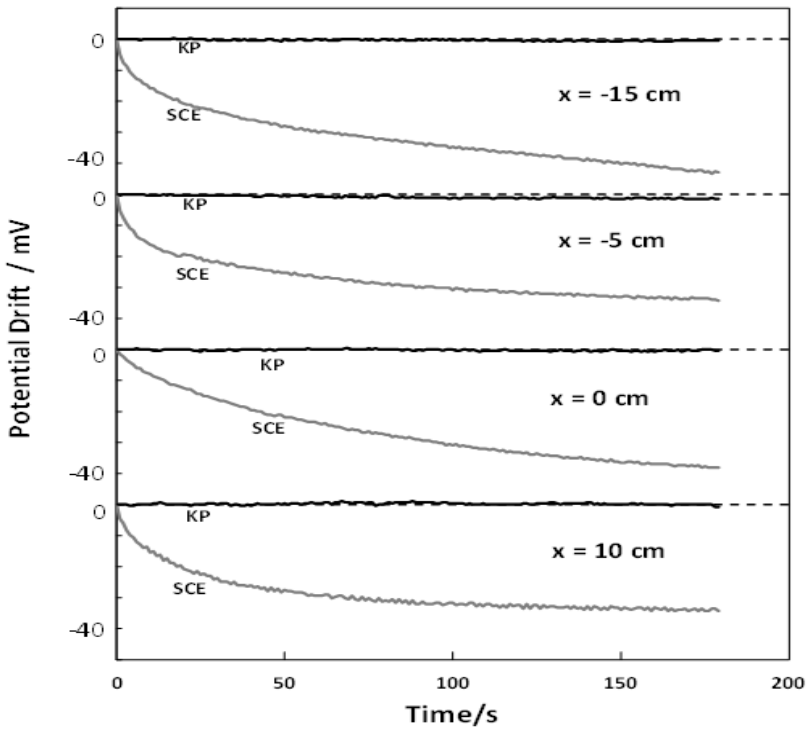

Figure 2: High stability of measured potential with KP compared with conventional electrode (Saturated Calomel Electrode, SCE), shown by drift from value measured 1 second after each probe placement on a dry, undisturbed concrete surface. Tests for four positions away from center of a test slab. Adapted from Sagüés and Walsh [*11*].

Potential profiling capability: The laboratory trial tests also demonstrated that the KP can produce potential profiles similar to those obtained with conventional electrodes, but without need for surface contact or conditioning. Figure 3 shows profiles obtained on a reinforced concrete slab having a rebar with a central corroding spot. The shape and range of potential profiles measured with the KP were consistent with the location of the local corroding anode in the slab. Within a given slab, the KP measurements in the dry (undisturbed) concrete surface condition showed excellent reproducibility. The KP profiles were offset from, but comparable in shape and range, to those obtained independently with a conventional wet-tip reference electrode that had been allowed to stabilize. The offset depended on the condition of both the KP disk and the concrete surface, indicating that appropriate calibration is needed if absolute potential determination with the KP is desired. Comparable KP profile features were obtained when sampling the concrete in either the dry or a pre-wetted surface condition, demonstrating the probe's ability to identify a corroding location.

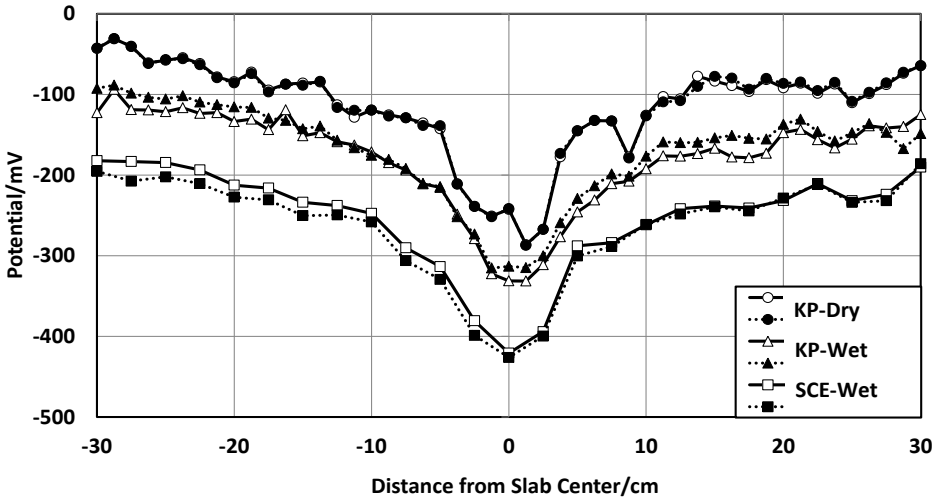

Figure 3: Laboratory tests demonstrating the ability of the contactless KP to identify the position of a corroding spot on the center of a test slab with either a dry or wet surface. Results are similar to those obtained with a conventional, contacting wet-tip SCE electrode). Adapted from Sagüés and Walsh [*11*].

How the KP May Be Applied in a Future Fully Developed System

Based on the encouraging performance of the probe in the initial laboratory trials, the work in this Type 2 NCHRP-IDEA Project acted on selected issues for the implementation of the concept for field application.

The selected issues addressed in this project are presented in the next section. However, before proceeding and to establish the proper context for the proposed work, a conceptual description of a possible production system (as it may be commercially implemented after completion of this project) is given next. It is envisioned that a future production system will eventually incorporate features such as those shown in Figures 4 and 5, illustrating a bridge deck survey application as it holds promise for being the most suitable for initial implementation. The system would feature a lane-wide traveling array of multiple probes perpendicular to the lane direction, mounted on a small trailer cart pulled by a slow moving vehicle. Production units should include a brush sweeper or similar mechanical guard ahead of the array to divert any loose debris on the deck surface, and safeguards such as auxiliary wheels on the sides of each individual sensor to prevent it from damage by contact with any deck surface high points. Construction should be modular with easily replaceable spare components. A data logger would record the potential readings from each probe as the array samples the entire bridge length. Following the usual practice in conventional potential surveys, the results can then be instantly summarized in a color-coded map identifying any highly negative potential spots indicative of ongoing corrosion. Operation of such a system could occur in two alternative modes, Absolute and Differential.

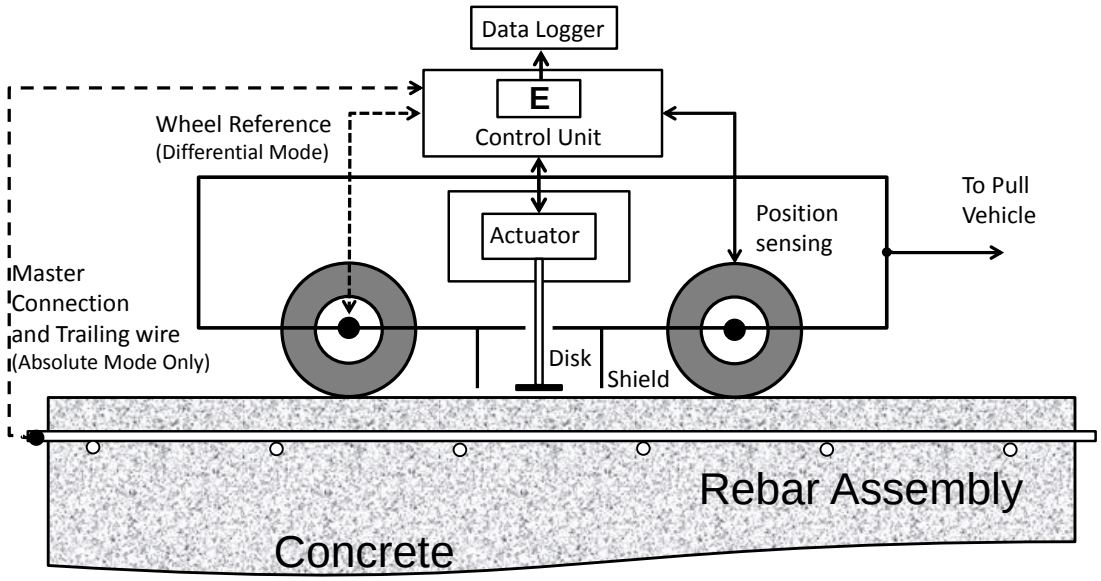

Figure 4: Anticipated features of a future production system; side view. (Patent pending on all graphic material related to devices presented in this report.).

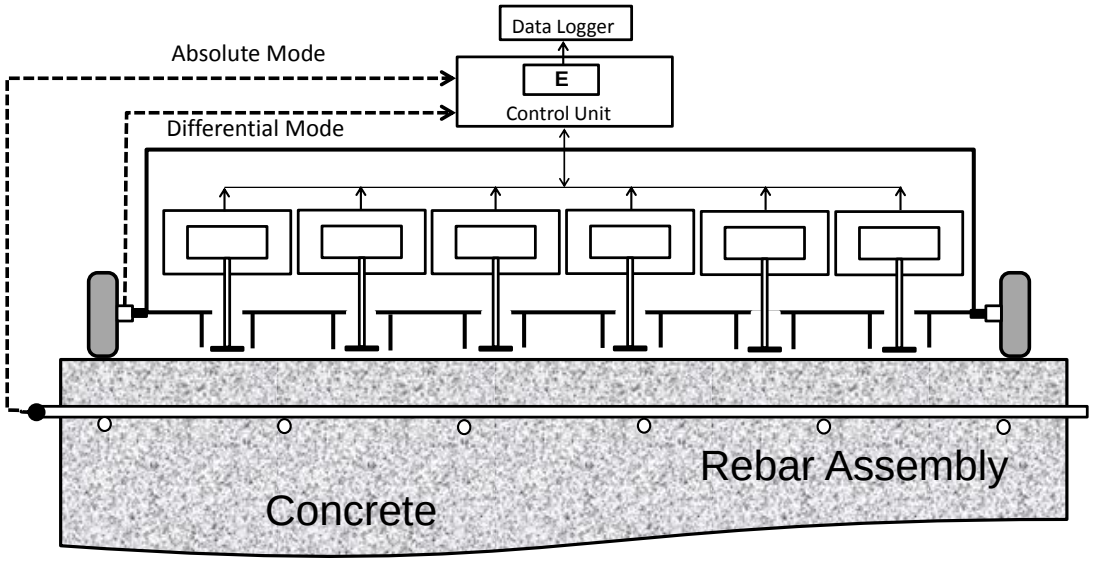

Figure 5: Anticipated features of a future production system; front view.

An Absolute mode, as in traditional potential surveys, would use a wired master contact from the probe casings to the deck rebar assembly. The contact can be prepared by operators ahead of the survey by exposing reinforcement at one spot on the side of the road and attaching a contacting stud, which can be left in place for future inspections as well. A trailing wire connects the master contact to the cart as it travels the

length of the bridge corresponding to the rebar assembly being sampled. This mode, with suitable calibration of the reference disk material to a conventional electrode, may yield potential readings that can be compared in absolute terms with those specified in ASTM C-876 [*4*] to estimate the likelihood of ongoing corrosion. This mode was demonstrated in the present project as detailed in Section 4.2.

A Differential mode would be a more attractive alternative from the point of view of operation speed. This mode does not require a trailing wired contact to the rebar assembly and the rolling system is completely self-contained. The casings contact to the rebar is replaced by a sliding contact to a tire in the trailer that is surfaced by electrically conductive rubber. The potential readings provided by the probes in the array are in this case referred to the surface potential of the wheel contacting surface. However, the nature of that contact does not matter as it is nulled out by the circuitry so that only the differences between the potentials of the disks in the various probes in the array are recorded. An additional probe or wheel is also needed to keep track of potential references in the lane direction. This mode cannot provide absolute potential readings but yields instead a relative potential map, referred to as an arbitrary point on the surface of the deck. Such information can nevertheless identify zones in the deck with significantly more negative potential than the rest, indicative of ongoing corrosion in those zones. The differential mode may be also of use for surveying decks constructed with epoxy-coated rebar (ECR), where the assembly is not reliably interconnected. While interpretation of potential maps for ECR is subject to considerable uncertainty [*15*], variation of potential patterns with time in successive assessments may provide an added tool for nondestructive detection of corrosion there. This mode was conceptually explored in this project as detailed later on.

These systems could be readily adapted as trailers to other instrumented diagnostic vehicles already owned or contracted by the state transportation agency.

4. INVESTIGATION

General Objective

This project developed and demonstrated a KP device that samples the surface of reinforced concrete with a novel contactless electrode, providing rapid and stable electrode potential mapping for early corrosion detection in highway structures.

Approach and Stages

The trial experiments detailed in Sagüés and Walsh [*11*] demonstrated that a KP for scanning surface concrete potentials was feasible under ideal laboratory conditions. However, success of the probe in field conditions needed resolution of several remaining issues, which were addressed by the project stages shown next. The scope of the stages is shown as conducted, reflecting redirection of some of the work as technical priorities and feasibility of approach became better defined.

Stage 1

Work in this stage focused on scaling up from an existing stationary miniature proof of concept version of the device, to a mobile and practical large size unit suitable for realistic road conditions. Three interrelated activities were conducted. In the first activity, the probe sensing disk and operating gap were scaled up to dimensions (e.g., 10 cm and 1 cm to 2 cm, respectively) and ruggedness suitable for use on a typical bridge deck environments. The electro mechanical driving unit and electronic control system was scaled up accordingly. In the second activity, a wheeled platform with automatic operating gap distance control was designed and constructed to hold the probe and achieve adequate operating gap distance. The third activity integrated the outcomes of the other two by constructing a working single-probe prototype and optimized the combination of vibrating frequency, signal processing response time, and gap distance to increase usable speed of travel of the prototype. Test runs with the prototype were conducted on a laboratory platform. Platform trials in this project were limited to low, hand drawn speeds (e.g., 1–5 mph), but did however identify factors that will need consideration in determining the maximum expected speed of production units, and manipulate those factors for optimization. An alternative vibration-less translating probe mode was explored as a means to allow for faster scanning speed. Technology transfer contacts were established with the Long Term Bridge Performance (LTBP) program to discuss integration of the KP in robotic bridge deck assessment units.

Stage 2

Work on this stage first demonstrated coordinated operation of probes for effective potential mapping and field operation. Two activities were conducted. In the first, an array of two independent probes was constructed and made to operate jointly in a wheeled platform in Absolute mode (i.e., with one master wire connection to the rebar assembly), demonstrating coordinated operation and processing of data. In the second activity the probe array was operated on a decommissioned bridge deck at the Sunshine Skyway Bridge in Tampa Bay, Florida, in an aggressive marine service location and experiencing deck corrosion. The tests were conducted in cooperation with the Florida Department of Transportation (DOT). Potential maps were obtained using the KP array and compared with results from using conventional reference electrodes in the same locations. This activity also examined to what extent the KP application was sensitive to variations on concrete surface condition from moisture, contaminants, and other sources of artifacts.

4.1 STAGE I FINDINGS

4.1.1 First activity: probe scale up

A target 10-cm-diameter galvanized steel mesh design was selected. A mesh disk has advantages over a solid disk in this application: a lower mass that enables higher vibration amplitude, less air drag, and a reduced fanning effect on the concrete surface. Ensuring that a mesh disk has sufficient capacitance for appropriate operation was investigated in the early stages of the project. Calculations and tests (Figure 6) showed that at small gaps a mesh disk was nearly electrically equivalent to a solid disk of the same diameter [*15*].

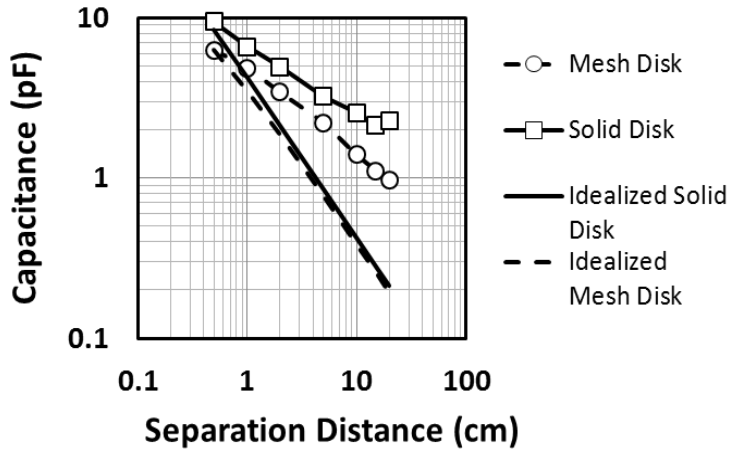

Figure 6: Illustration of the relationship between the separation distance of a solid and mesh disk and a parallel plate. At relatively small gaps the capacitance is sufficiently high.

Design of the sensing disk focused on ensuring that the disk vibrated with a uniform profile. To that end a secondary mesh was soldered on as reinforcement. A basic engineering approach was followed to achieve structural stiffness by increasing area moment of inertia [*16*]. A crosshatch reinforcement layout was thus implemented as shown in Figure 7. Upon testing, this reinforcement configuration proved to be sufficient in preventing undesirable nodal vibrations.

The disk was attached by a central screw to a 10-cm-long, 8-mm-diameter wooden stem. Wood was chosen to minimize any triboelectric static charge generation during vibration [*11*]. The stem was connected to a Pasco Scientific Model SF-9324 voice-coil mechanical vibrator. The vibrator was driven by one channel of a consumer-grade audio stereophonic unit, to which the vibration output of the KP electronic control unit (same control unit as in Sagüés and Walsh [*11*]) was connected. A larger capacity electronic driver was used later on for the field tests.

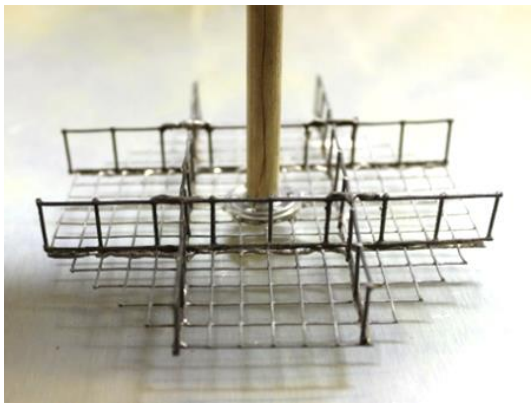

Figure 7: The final 10-cm-diameter sensing disk, constructed from 6.3-mm galvanized steel mesh.

After construction, testing was conducted to demonstrate the functionality of the scaled-up sensing arrangement on laboratory concrete slabs. For initial testing the scaled-up sensing arrangement was mounted in a stationary manner with a movable specimen underneath (Figures 3 and 4).

Two available concrete slabs (Figures 8 and 9) were used, each 70 cm long, 15 cm wide, and 5 cm thick, with one #3 (1.3-cm-diameter) steel rebar placed longitudinally on center. The concrete in the central ~5 cm of the slab was contaminated with Cl- ions to induce active corrosion of the rebar there, while the rest of the rebar surface remained in the passive condition. Detailed description of the slabs is given in Sagüés and Walsh [*11*].

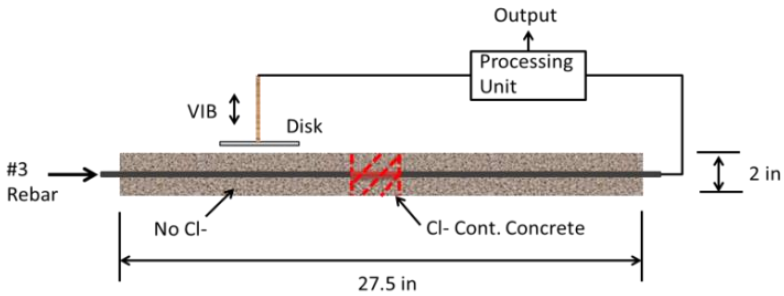

Figure 8: Schematic of the laboratory experimental setup.

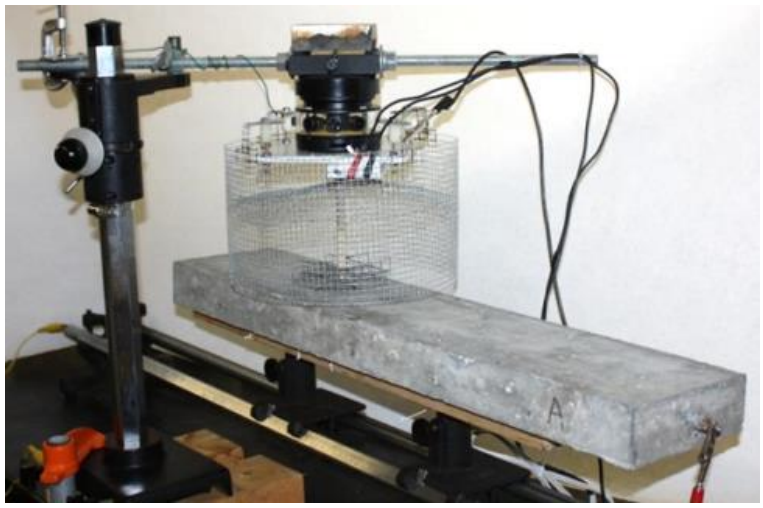

Figure 9: Laboratory concrete slab test setup. Rebar and its connecting point are seen emerging at right end of slab. Disk assembly is stationary, while longitudinal position is changed by sliding slab over the graduated rail. The sensing disk is surrounded by a grounded wire mesh electric shield ~25 cm in diameter. Vibrating assembly is located at top; wires connect system to electronic driving and signal processing unit.

The disk was positioned over the longitudinal centerline of the surface of the slab as shown in Figure 8. Vibration frequency in these tests was 80 Hz and vibration amplitude ~ 1 mm. The disk-to-concrete surface distance was 1 cm and 2 cm for different test series. Potential readings were taken at 13 longitudinal positions at 5 cm intervals, starting with the left disk edge directly above the left end of the slab. Disk position was recorded as the distance along the disk axis from the left edge of the slab; slab center (corroding region) was thus at disk position= 35 cm.

The tests were performed on the two replicate slabs and on both the top and bottom of each slab. After the tests were finished on each side of a slab, an additional set of traditional-method potential readings was taken at each position using an SCE fitted with a moist sponge at the tip. KP readings were taken within ~5 seconds of placement at each new position. SCE readings were taken after waiting ~15 seconds after sponge contact with the concrete to allow for a uniform degree of approach to stabilization of the potential, which for the traditional method is subject to drift as noted in Sagüés and Walsh [*11*].

Results for tests conducted ~ 1 day after removal of both slabs from their 100% R.H. storage container are exemplified in Figure 10 for the top-side potential measurements of each slab. Bottom-side results were comparable to those shown here. The results demonstrate that the scaled-up KP sensing system was functional over concrete surfaces and able to identify for both slabs the central corrosion location via the lowest point of the potential profile. The identification was consistent with that of the traditional method using the wet-tip SCE. The offset between the KP and wet-tip electrode potential readings was generally consistently uniform and suitable for calibration of the KP if absolute potential measurements were desired. These findings are in agreement with those obtained for the miniature KP system used while initially developing the concept [*11*].

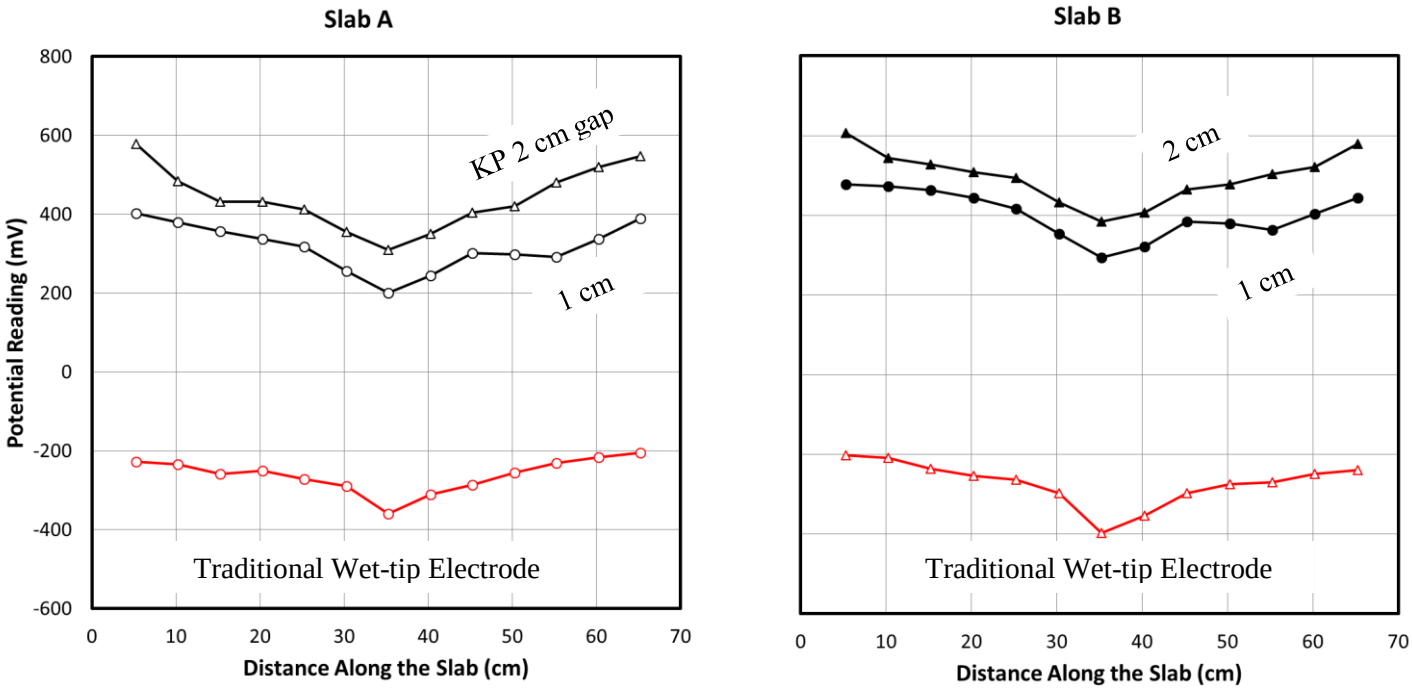

Figure 10: Potential scans in replicate slabs obtained with the KP operating at two disk-to-concrete surface gaps [1 cm and 2 cm (~ ⅜ in. and ¾ in.)], and with the traditional SCE wet-tip electrode method. The corroding region was located at the center of each slab (35 cm position)

The results also demonstrated that the KP was able to operate successfully at an appreciably large, 2 cm gap (20 times greater than that used in the initial miniature unit) between disk and concrete surface. This finding was important as the ability to operate with a gap of such size, which is significantly greater than the typical short-term deck surface roughness amplitude, was a necessary requirement for practical use of the product of this project. It is also noted that the KP was able to show good spatial resolution with a sharp minimum potential location even though the disk diameter was equal to two sampling spaces, and even when operating at the 2 cm gap. This observation indicated that the sampled footprint was reasonably confined.

The potential measured by an ideal KP should not depend on the height of the operating gap, but in practice residual capacitive coupling between various parts of the system tend to introduce some gap size sensitivity [*11*]. The results in Figure 10 showed that the potential profiles for 1-cm and 2-cm gap sizes were offset from each other by a nearly fixed value of ~100 mV while retaining similar shapes, suggesting that a potential-to-gap functional dependence of ~0.1 V/cm existed at least for the potential and distance ranges examined then. An important outcome of that observation was that it would not be necessary to perform fine physical real-time control of gap distance when a vehicle-mounted probe is moved over the deck surface. Rather, an auxiliary disk-to-concrete distance sensor could be used to provide real-time topography information as the concrete surface is scanned. That information could then be applied, if necessary, to numerically correct the probe potential readings to compensate for gap variations once a preliminary functional dependence was established beforehand. Consequently, during the execution of this project, gap control was limited to that achieved passively by simple use of a short wheel base, as done for the wheeled platform described later. Moreover, in Stage 2 of the project, the use of an active shield biased to an adequate

adjustable potential permitted eliminating much of the residual sensitivity of the potential reading to the operating gap. Thus, while the capability for post-processing correction of potential readings based on the measured gap record was kept in place, it was relegated to a selectable optional adjustment that was not activated during the field tests.

Short-term reproducibility tests were conducted by performing multiple consecutive profile measurements on one of the slabs, with results shown in Figure 11.

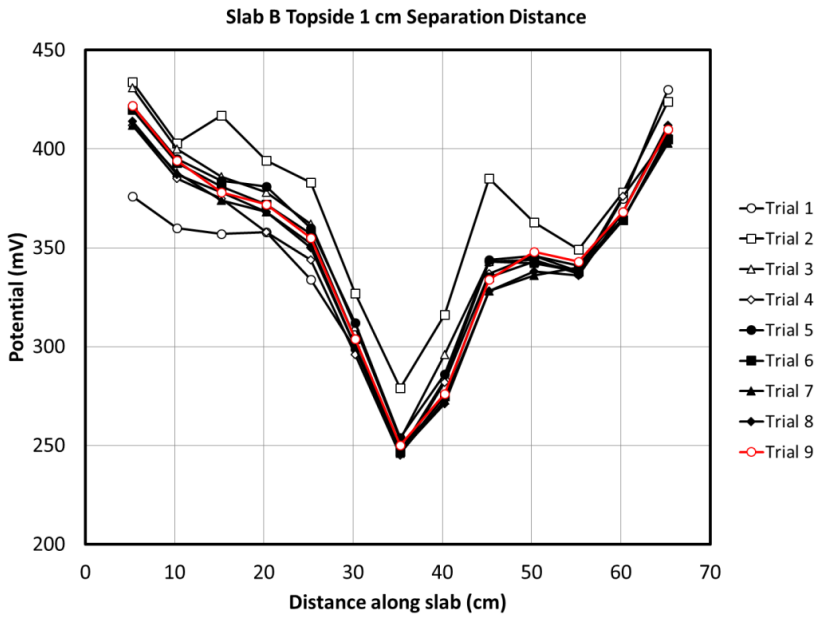

Figure 11: Short-term reproducibility tests. Vertical scale expanded to emphasize test-to-test deviations.

The tests revealed that under the present implementation there was a good degree of reproducibility of potential scans, providing identification of the corroding spot in all trials. The average standard deviation around the average of the entire set of nine potential readings obtained at each position was only ~12 mV. However, the tests also revealed some instances (trials 1 and 2) where some temporary and nearly uniform potential reading offsets occurred over some of the slab positions tested. The average standard deviation for the rest of the trials was only ~5.3 mV.

4.1.2 Second activity: integration in a wheeled platform

A robust prototype wheeled platform (Figure 12) was designed and constructed in the shape of a 30 cm cube, using standard 41 mm of Unistrut ™ metal framing and fittings, with an arrangement of three 10-cm-diameter wheels for triangular base geometric stability.

Per the outcome of the previous item, gap control was achieved passively by the short wheel base of the unit, which was amply sufficient for the outdoor tests (next section) that were performed on a well-

screeded slab surface. The platform was connected to the control unit by a flexible 6 m long cable. The platform included a removable shield around the disk.

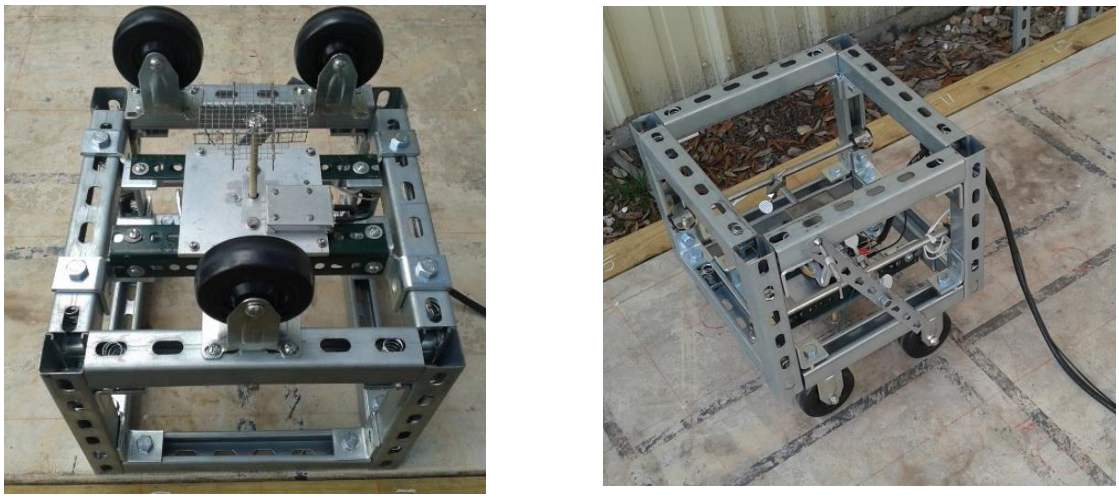

Figure 12: Wheeled platform for Stage 1 tests.

4.1.3 Third activity: test runs with the prototype conducted on an outdoors platform

An existing instrumented reinforced concrete square test slab approximately 2.3 m x 2.3 m x 0.14 m (Figure 13) was adapted for the present project with the addition of a surrounding wood skirt, so that the entire upper concrete surface can be covered by the sensing disk by movement over the platform wheels. The instrumented slab contains an array of 15 #4 steel rebars equispaced 15 cm on center, beneath a 9 cm clear concrete cover. Each bar is capable of individual electrical connections and four of the bars are further electrically divided into shorter segments. No chloride ions have been added to the concrete.

Figure 13: The reinforced concrete slab has embedded rebar segments that are internally isolated so as to allow various combinations of cathodes and anodes to be designated based on external electrical connection.

The arrangement allows, by means of an external current source, to temporarily convert different parts of the system into anodic or cathodic regions, thus simulating a wide variety of equivalent corrosion location scenarios with corresponding actual potential distributions on the top surface. Those potential distributions can then be sampled with the KP or with conventional electrodes, creating a variety of data sets to evaluate and demonstrate probe functionality.

For the testing, two bar segments, each ~1 m long, were wired as anodes and the remaining bars were made cathodes (Figure 14). By use of a large controlling resistor and a relatively large driving potential (9 V) the system operated under quasi-galvanostatic conditions. Temporary anodic current densities representative of a fast corroding anodic spot were used.

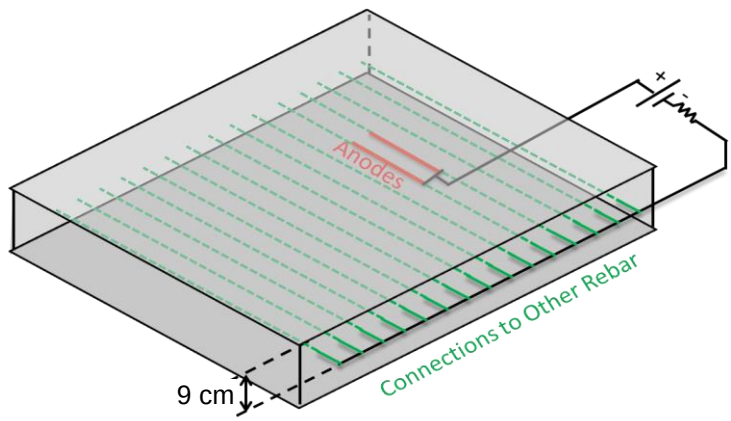

Figure 14: Connection configuration for tests.

The wheeled probe performance was evaluated in two conditions, described in Table 1, Condition 1 was evaluated in December 2014, when the electronic control unit required a relatively long stabilization time (~15 seconds), and when operation required a floating potential condition for the rebar assembly as it had been used for laboratory tests. Condition 2 was evaluated in March 2015 after considerable KP control unit improvement to reduce stabilization time to ~1 second, and to permit testing a fully grounded rebar assembly as it is the case in a regular bridge deck system. Gap distances were modest in these initial tests, but still comparable to those that may suffice for not too rough realistic concrete surfaces.

Table 1 Outdoor Slab Test Conditions

Condition	Disk-Concrete Gap Size	KP Vibration Frequency	KP Stabilization Time	Rebar Assembly Grounding	Impressed Current Density at Anodic Segments
1	0.6 cm	81 Hz	15 s	Floating	2 μA/cm^2
2	1 cm	157 Hz	1 s	Fully Grounded	3 μA/cm^2

For each condition the tests were also made with the rebar assembly in the unpolarized, all-rebars-shorted mode, simulating a bridge deck with no corroding spots. In each KP run the potential at the crossings of a 0.3 m grid (approximately in register with the 0.15 m rebar spacing) traced on the slab were scanned sequentially, moving manually to the next crossing after waiting for the indicated stabilization time. Furthermore, after each KP scan was finished the same scan was performed with a regular CSE reference electrode fitted with a wet sponge at the end, waiting about 10 seconds for stabilization at each test point. Results of both test conditions are presented in Figure 15.

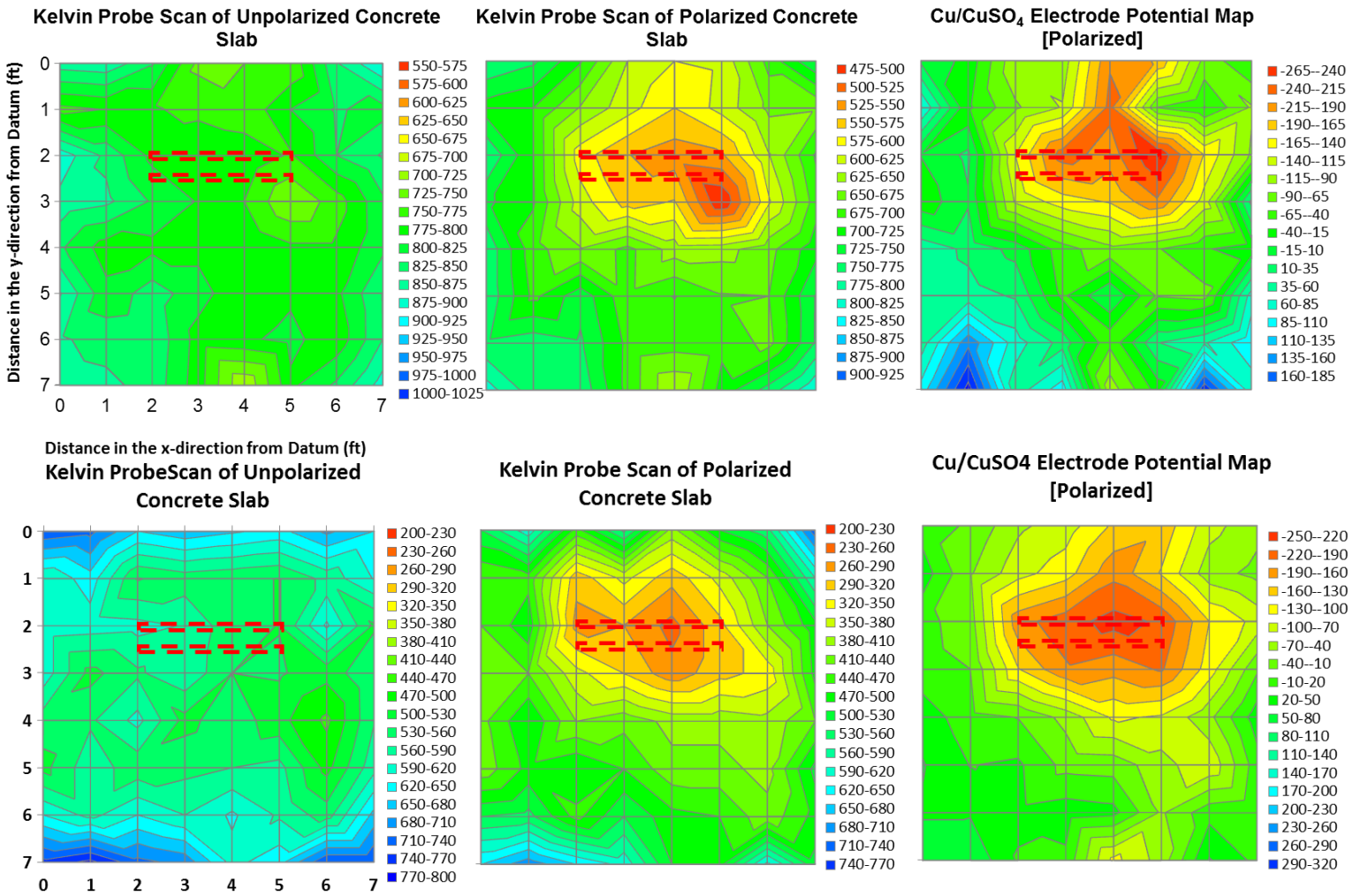

Figure 15: Results of outdoor rebar tests for Condition 1 (top) and 2 (bottom). The location of the anodic segments is indicated by the dashed red outlines.

The results were highly encouraging. In the absence of rebar polarization the KP showed as expected a flat potential profile, in agreement with that obtained with the CSE electrode in the same condition (not shown). On the polarized system the contactless KP measurements showed a distinct differential potential profile identifying the position of the temporarily anodic segments, and in excellent agreement in both locations and high-to-low potential difference in the comparable profile obtained with the traditional CSE method. Figure 16 is a graphical representation of that comparison, showing how for the reference disk material used (galvanized steel) a nominal calibration offset of 715 mV could be used as a simplified single-parameter means to translate the KP readings to comparable CSE measurements.

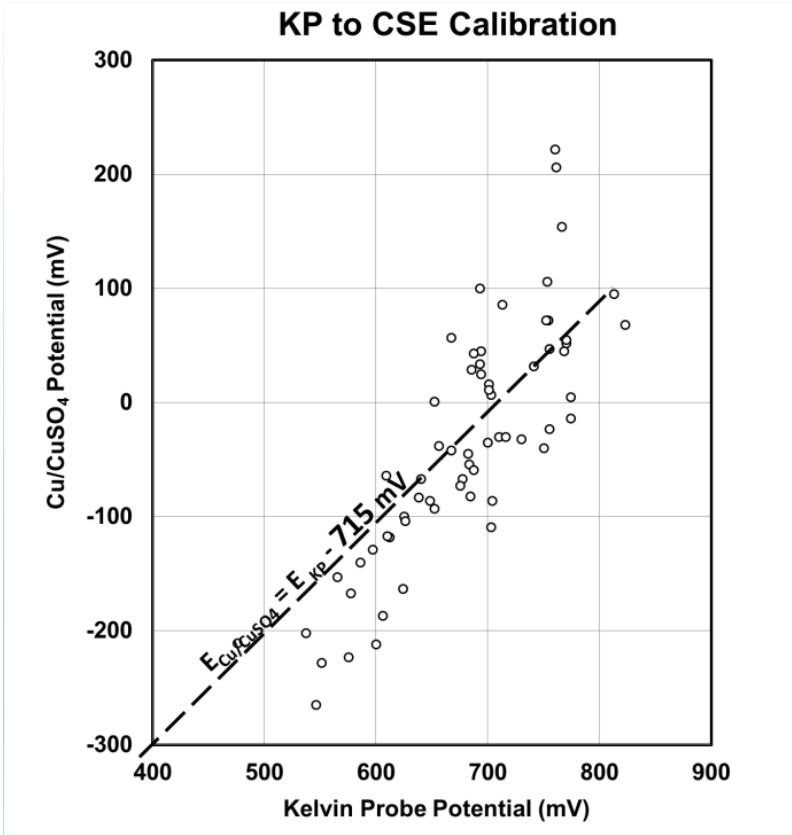

Figure 16: Comparison of potential values obtained in the Condition 2 test for the KP and the CSE on the same test points.

It is emphasized that that offset value is for the specific condition examined and not a universal translation parameter. The precise value will depend on disk material used and other items that were further evaluated during Stage 2 of the project. Also, as noted in discussion of Stage 2 findings, for both the KP and the CSE data a certain amount of experimental scatter exists, as it is well known that interpretation of potential maps requires consideration of the entire map and not on single individual values.

As part of this Stage 1 activity, initial estimates of feasible operating regimes for a KP as part of a moving vehicle or trailer were made using simplified considerations. It is expected that to give a useable signal a KP vibrating disk should be over a given test spot for an amount of time corresponding, in the extreme, to at the very least about 1 vibration cycle. Experience with the laboratory units [*11*] indicated that measurements spanning on the order of ~100 cycles provided highly reliable results. Hence, a minimum numbers of cycles Nm somewhere between 1 and 100 (marginally possible and well-established outcome, respectively) might be sufficient for practical operation in the field. The amount of time passed during Nm cycles is $tc = \mathrm{Nm}/f$, where f is the vibration frequency. If the vehicle moves at speed v, the distance P travelled during that time is $P = v\ tc = v\ \mathrm{Nm}/f$. Typical bridge deck potential surveys tend to reveal details on the order of 1 m in size [*17*]; a somewhat ambitious target of 0.3 m resolution will be considered in the following. The maximum operating speed S_m that would make P = 0.3 m (i.e., to have a good chance of revealing the presence of a differentiated potential region as small as 0.3 m) is then given by:

$$S_m \text{ (km/h)} = (P(m))/(t_c\,(s))*3.6 \qquad \text{Eq. (1)}$$

where the factor 3.6 adjusts for the conversion between the units chosen. Figure 17 graphically represents the application of Eq. (1).

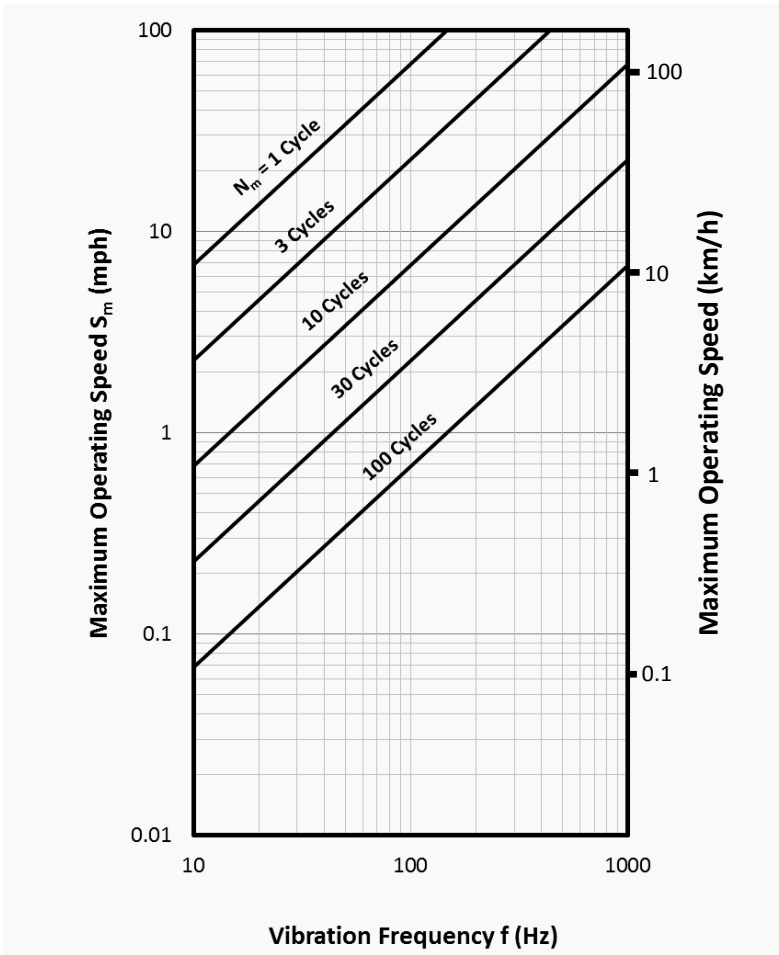

Figure 17: Estimated maximum operating speed for 0.3 m features resolution as a function of disk vibration frequency and number of cycles required for a useful reading. Speed in customary units included as well.

It can be noted that within the scope of this project, demonstrations of probe functionality were to be limited to hand-drawn platforms, which implies scanning speeds somewhere in the 1–8 km/h range. Nevertheless, Figure 17 allows for examining various possible scenarios in future optimization. For example, if the number of vibration cycles needed for reliable results were 10 (in the logarithmic center of the range mentioned earlier, possibly achieved by sophisticated signal processing), and the operating frequency ~150 Hz (as in the outdoor trial addressed earlier), the maximum speed would be that of a slow moving vehicle, about 10 mph. Operation with a 10 cycles acquisition lapse at 64 km/h (typical minimum interstate highway speed) would require vibration frequencies approaching 1 kHz. Such operating frequency is within the realm of the

possible as well, but would require further development in designing the disk and electromechanical or alternative drivers. For the purposes of this project, the operating frequency of ~150 Hz has been retained and optimization of the data has been addressed primarily by means of the deconvolution procedure described in the Stage 2 findings.

Finally, a radically alternative means of operation would consist in using a non-vibrating disk and monitoring only the electric charge changes that take place when moving the probe at a fixed operating gap over different potential regions on the bridge deck surface. In such case the operating speed has actually a minimum value, dictated by the sensitivity of the sensing front end circuitry and the amount of electrical noise inherent to the system. Precise gap control or gap measurement would be essential in that concept. This issue pertains to future development in subsequent investigations.

4.2 STAGE 2 FINDINGS

4.2.1 First activity: Design and construction of an operational dual KP array

In fulfillment of Stage 2 objectives, the single KP developed during Stage 1 of the project was duplicated and the two units integrated as a dual KP array capable of synchronized operation. Design included migration from the analog electronics signal processing and control unit used in Stage 1 toward a digital-based system. Compact power electronic units for vibrator operation were selected and acquired to replace the bulky consumer electronics stereo amplifier used in the initial tests. A position measuring wheel prototype was designed and constructed by Dr. M. Celestine of USF Engineering Technical Support Services for integration with the Stage 1 prototype and acquisition of position information for automatic potential mapping.

The dual probe array was built on a robust wheeled platform, with both probes including some improvements over the KP unit developed under Stage 1. Those improvements were:

- Improved software control. With the exception of low level signal processing by an analog electronic front end connected to each disk, followed by an analog 60 Hz filter and analog 100X amplifier, all other probe signal processing is conducted digitally by a laptop PC, using a LabVIEW ™ platform. The PC also generated the excitation signal for the vibrating solenoid via an analog power amplifier. All functions are battery operated and operated mobile onboard. The physical unit is shown in Figure 18.
- Incorporation of an electric shield around the vibrating sensing disk.
- Addition of a compensating DC potential bias to the shield to minimize spurious vibration-induced signals resulting from differences in work function between the shield and the disk materials. This function also minimizes sensitivity of the read potential to variations in the disk-concrete operating gap.
- Configuration of the shield as an active shield so that it tracked via a voltage follower any potential changes of the sensing disk during automatic zeroing operation and added those to the compensating bias, thus allowing for the compensating bias to remain effective over a wide range of measured potentials.

- Continuous disk-concrete operating gap distance measurement, obtained simultaneously with the KP potential measurement. Gap measurement was made by adding a constant amplitude 2 kHz AC potential to the zeroing KP signal. The corresponding capacitive current between the disk and the concrete was separated by filtering from the imbalance signal generated by the probe's front end, and the root mean square value of that current was measured. The capacitive current value is inversely proportional to the gap size, and the gap size was obtained accordingly, following a simple calibration procedure where the disk was placed at two known distances from the concrete surface. The appropriate conversion constant and formula is then stored in the operating code for the system, so that the instantaneous gap value is displayed in the operating screen and stored continuously in the output file on command. The gap value record can be used to adjust on post-processing for any residual uncompensated sensitivity of probe reading to gap distance variations. Although this post-processing feature was not enabled in the field tries, it is available for future development.
- Adjustment of control program feedback loop constants to minimize response time while preventing instability oscillations.

The dual probe array was initially fitted with 10-cm-diameter wheels (for the first field test), which were subsequently enlarged to 15 cm wheels for greater stability and used in the second field test. The array has two redundant linear position measurement devices. Each device is attached to a different wheel in the three-wheel mount. One device is a robust unit with a magnetic sensor having 8 cm resolution. The other device has 1 mm resolution. Mechanical stops permit rapid transition between 1 cm and 2 cm disk-concrete gap operation.

Figure 18 shows the dual probe array being operated during the field tests, and Figures 19 and 20 shows the lower portion of the unit.

5/19/16 7/27/16

Figure 18: Field probe operations at indicated dates. Note larger wheels for the second test date.

The dual probe array was moved by pushing at a typical speed of 0.6 m per second or about 2.2 km/h. Normal bridge deck roughness resulted in only moderate vibration of the system and operation for cumulative distances on the order of hundreds of feet took place without any mechanical malfunction, despite the unit suspension not having any springs or shock absorbers, which could easily be implemented in a commercial production unit.

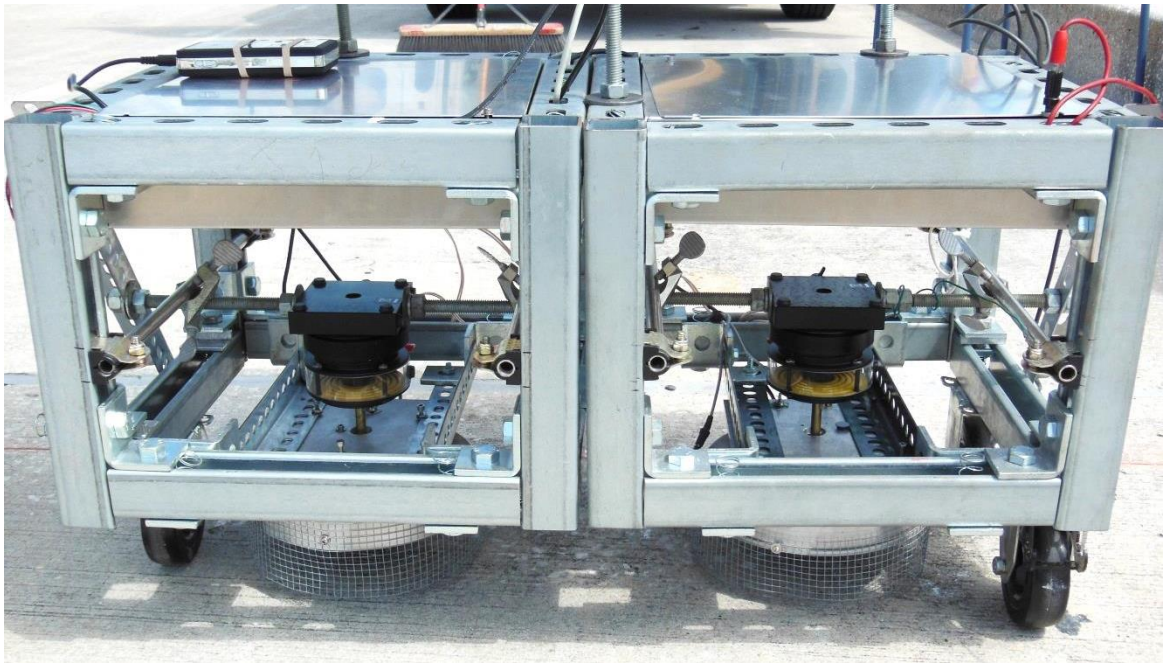

Figure 19: Lower portion of the dual probe array (as configured for the May 19, 2016, test, with 10 cm wheels) showing the vibrator drivers and the active shields around each sensing disk.

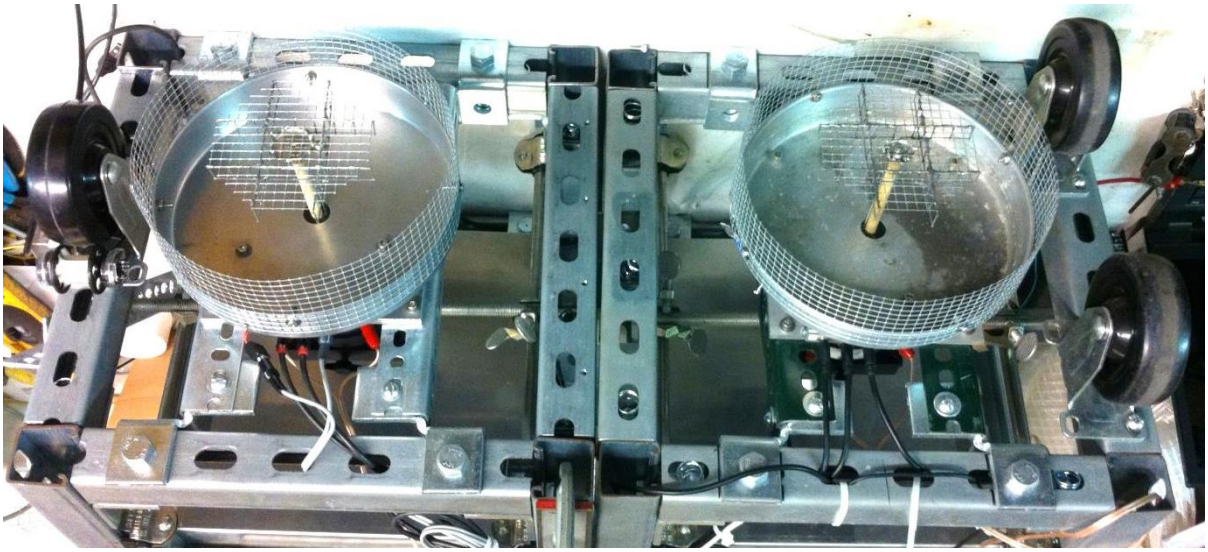

Figure 20: View from underneath the dual probe array showing the sensing disks with surrounding active shields (wheels as in the May 19, 2016 test).

4.2.2 Second Activity: Field Tests

4.2.2.1 Field Test location and scope

A ~50-year-old section of the North Skyway Fishing Pier, part of the former west access road of the old Sunshine Skyway Bridge in Tampa Bay, was selected for field tests of the dual KP array. The former west bridge access, designated as FDOT Bridge No. 159008, begun construction in 1966 as part of a 4-lane expansion project at the time[1]. The bridge deck region chosen (circled in Figure 21) is located on the east lane at the north end of span No. 44 of the former access, a convenient location close to a parking spot. The basic test space on the deck was a 2.7-m-wide, 5.5-m-long rectangular plane detailed in Figure 22. Hollow core drill holes to access the rebar mat were made by Florida DOT personnel at the locations denoted in Figure 22 as R1 and R2, where clear rebar concrete cover was determined to be 4.44 cm and 3.81, cm respectively. Original design plans specified an upper rebar mat of the deck of #5 rebar placed on 25 cm centers, with a clear cover of 3.81 cm; a lower rebar mat with both #4 and #5 rebar with a specified 4.44 cm clear cover, an overall concrete thickness of 17.8 cm and Class A concrete. After verifying that electronic continuity existed between the two locations, insulated wires were attached to the each exposed rebar and the holes were patched with mortar leaving a permanent short wire segment emerging from each patch. All the subsequent tests described in this section were performed using only the R1 wire connection.

Figure 21: North Skyway Fishing Pier.

[1] Not to be confused with an east portion of the old bridge access built in the 1950s, which was demolished starting in 2011. The fishing pier runs parallel to the low access portion of the new Sunshine Skyway Bridge, which was commissioned in 1987.

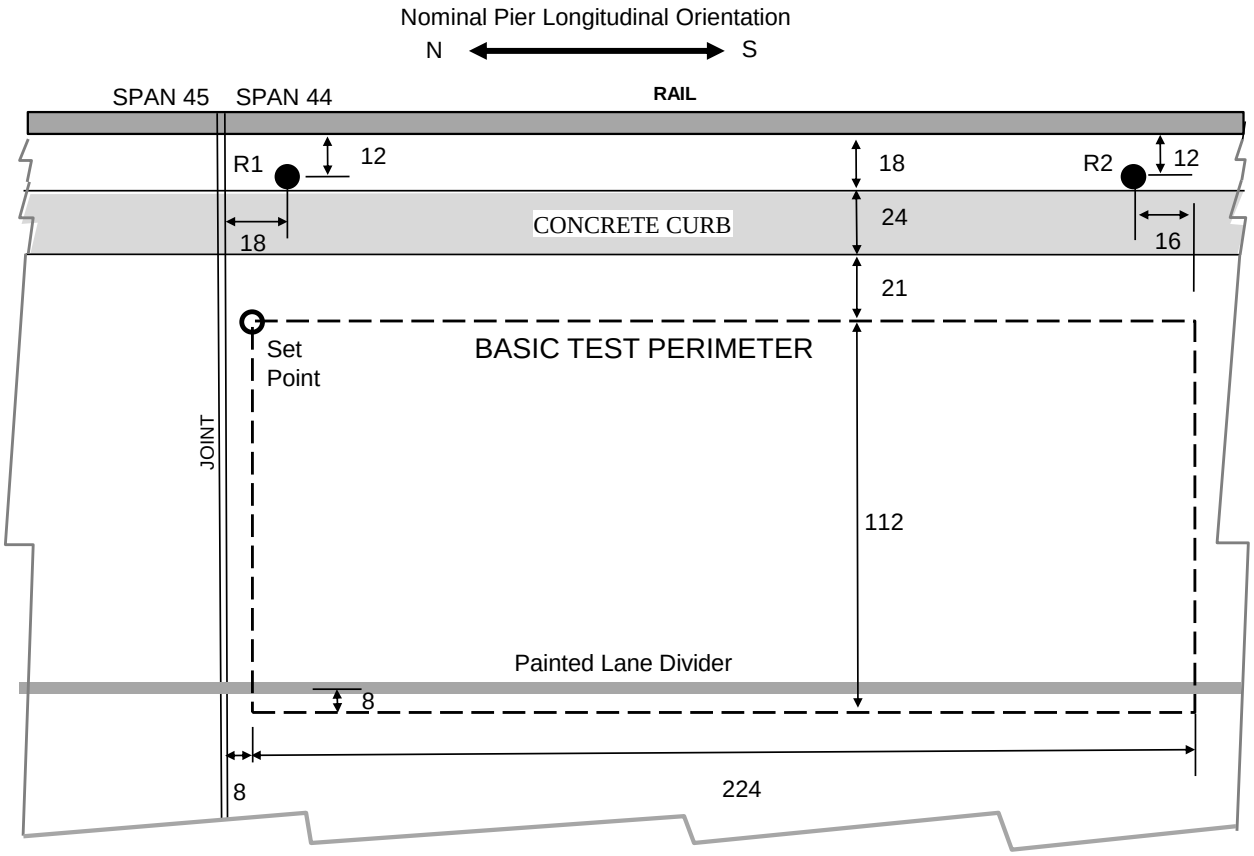

Figure 22: Test domain perimeter. Per practical reasons of field lay out, all dimensions are given in customary units (in.); 1 in. = 2.54 cm. R1 and R2 denote rebar access drillings.

As illustrated in Figure 23, the bridge deck surface in the domain examined showed some wear and minor roughness, but it was overall clean and with no conspicuous distress, cracking, or potholes.

Figure 23: Representative surface condition of the deck location near the lower left corner of the perimeter in Figure 22, showing the joint between Spans 44 and 45, painted lane divider, and chalked grid lines used to organize the CSE measurements and KP measurement laps. Contrast and color saturation were enhanced to reveal minor roughness and presence of transverse grooving.

Field testing of the dual KP array was conducted on May 19, 2016, and July 27, 2016. Weather records for St. Petersburg, Florida, indicate no precipitation the day before May 19, 2016, but thundershowers for the day before July 27, 2016. Weather conditions on both test days themselves were sunny, with minor breezes and with air temperatures reaching a maximum near 90°F. The tests were conducted between late morning and early afternoon, with no visible surface moisture on the sun-warmed deck surface.

4.2.2.2 Field test procedure

On both test dates the basic grid test domain was first characterized by duplicate conventional measurements with a CSE approximating the C-876 procedure, followed by KP array measurements of the same region, with the KP probes set at two operating gaps (1 cm and 2 cm) and testing in duplicate in each case.

On May 19, 2016 additional tests were conducted after the main series of tests by creating wet spots and small oil-contaminated spots on the deck surface and running the probe array over those regions.

On July 27, 2016 an exploratory additional KP evaluation was conducted by starting at the same position as in the regular tests but extending, in the South direction, the test domain length from 5.7 m to 11.4 m. A single perfunctory conventional CSE evaluation of the extended location was conducted as well at that time.

Before conducting the tests the surface was lightly broom-swept and line marks were snapped with a chalking string creating a grid on 0.406 m centers, as detailed in Figure 24.

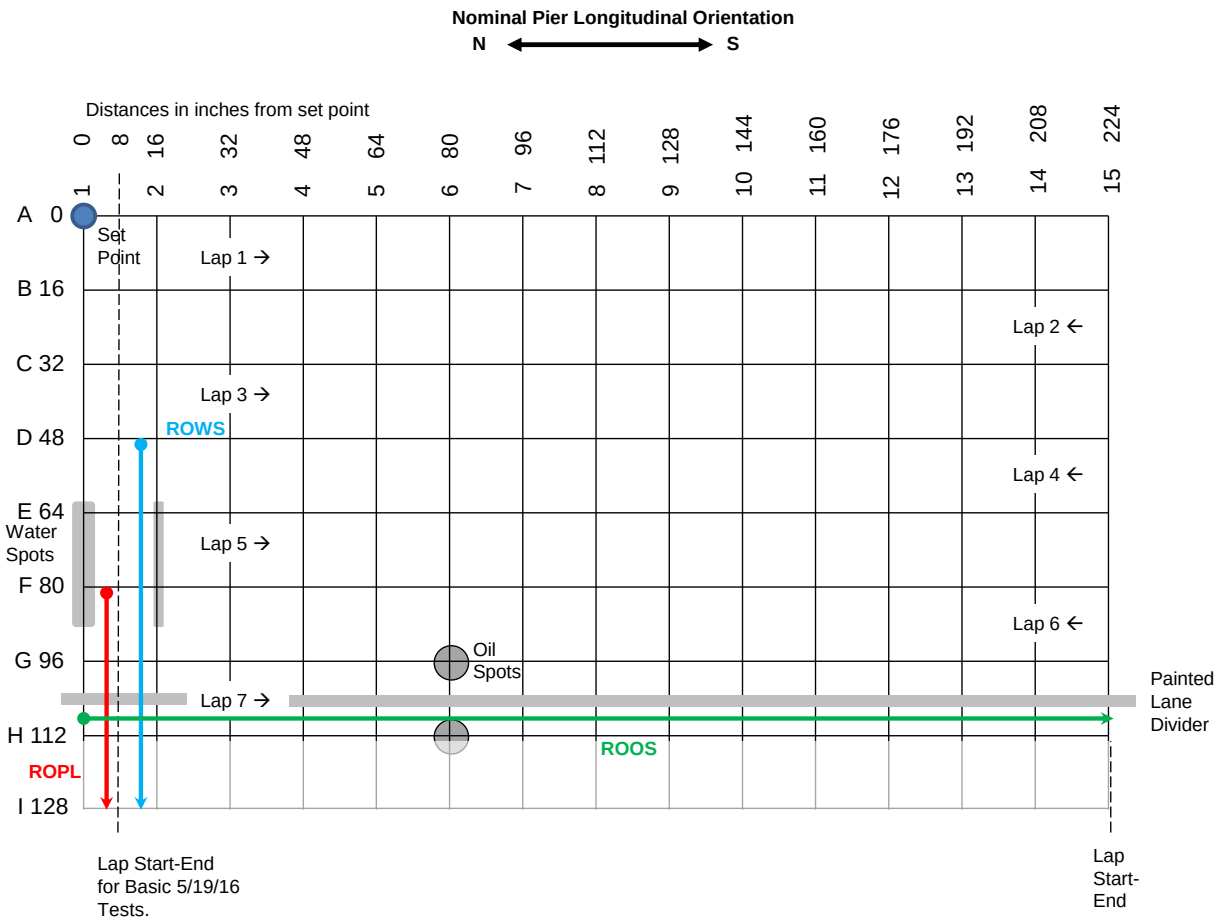

Figure 24: Basic test grid (A1 to H15) and KP lap pattern. Additional paths for ROOS, ROPL, and ROWS (see text) May 19, 2016 tests shown as well. Per practical reasons of field lay out, all dimensions are given in customary units (in.); 1 in. = 2.54 cm. Grid spacing is 16 in. = 0.406 m.

CSE potential measurements were performed on each grid intersection using a commercial CSE with a small sponge attached beneath the measuring tip and a high input impedance digital voltmeter. For each row in Figure 24, starting with the Set point (position A1) the sponge was wet with fresh water (no surfactant) and placed sequentially on each point and allowing for ~ 3 to 5 s stabilization time before recording the potential value and proceeding to the next point in the row. At the end of each row the sponge was rewetted and testing proceeded to the next row until the entire grid was covered. The duplicate test was conducted immediately afterwards.

For the basic May 19, 2016, tests dual KP array measurements were performed, starting with the array set to operate with a 1 cm gap, by first positioning the array so that KP sensor #1 was on the dotted line

indicated by Lap Start-End in Figure 24 at the left (north) end of Row A, and KP sensor #2 at the corresponding position at the north end of Row B, The data acquisition program was then started and the array was rolled by pushing it toward the South until sensors #1 and #2 were, respectively, on top of points A15 and B15. That data acquisition operation was designated as data acquisition Lap 1. The probe array was then manually displaced by one grid space in the west direction so that sensors #1 and #2 were on the B15 and C15 positions, and data acquisition Lap 2 was performed by rolling north until reaching the Lap Start-End line. The array was again displaced in the west direction to perform Lap 3 and so on until completion of Lap 7. Thus, redundant opposite-direction data sets were obtained for rows B–G, while rows A and H were sampled in only one direction. Typical Lap transit times were on the order of 12 s; counting the time for start/stop and lateral shifts the entire surface was covered in approximately 3 min. Instantaneous speed over the central ~80% portion of a given lap, after the initial acceleration and before slowdown in preparation to the final stop, was typically on the order of 0.6 m/s. After completion of a Lap sequence, the process was repeated to log a duplicate set of measurements. The dual probe array operating gap was then changed from 1 cm to 2 cm and the tests performed again in the same manner as before. Due to a recording malfunction, precise position data were only obtained for the 1 cm operating gap runs over the basic grid. For the 2 cm gap runs, the position was approximately derived from the simultaneous time records and an assumed time-velocity position based on the data for the 1 cm gap runs.

Additional tests conducted on May 19, 2016, all with a 1 cm operating gap included:

- Run Over Paint Line (ROPL) test: the dual KP array was placed on Row F and oriented so that sensor #2 was on position F1 and sensor #1 on F2. Array was then moved on a Lap that ended on Row I, causing the probe array to the cross paint line, which is between rows G and H. Probe array was then moved backwards (no lateral translation) in a second lap that ended back on Row F. The process was repeated in subsequent Laps.

- Run Over Water Spot (ROWS) test: Water spots approximately 0.3 m in diameter centered on positions F1 and F2 were created by spilling fresh water at each position. Laps were then immediately performed (with surface still visibly wet) as in the RPOL test but starting at Row D instead of Row F.

- Run Over Oils Spot (ROOS) test: Oil spots approximately 15 cm in diameter centered on positions G6 and H6 were created by spilling SAE 30 engine oil and then soaking excess oil with a towel. After waiting 15 min a Lap (O1) similar to Lap 7 of the regular mapping sequences (Probe 1 on Line G and Probe 2 on H) was performed. At the end of that Lap a return Lap (O2) was performed by reversing direction (no translation, each probe remaining on the same line as before). The process was repeated to obtain Laps O3, O4, O5, and O6.

The basic July 27, 2016, tests were performed similarly as in the previous date but with the Lap Start-End line coinciding with column 1 in Figure 24, thus covering a slightly larger area than before. The same start line was used for the extended domain tests, which lasted about 24 s per lap. For the July 27, 2016, extended domain tests the CSE grid over the extended section was placed on a 0.8 m center grid that was in register at the north end with the corresponding points of column 15 of the basic grid.

4.2.2.3 Field Test data organization and processing

The CSE data for each of the test dates were compiled and displayed on color-coded maps built using the averages of the duplicate potentials obtained for each grid point.

The KP data were obtained as a text file with a row for each acquisition time (each 0.1 second, so in the basic tests about 120 rows were recorded). Each row contained eight items: time, lap identifier, position along the measuring direction for each of the two redundant transducers, and for each sensor the gap size and potential measured. The data were subsequently parsed in a spreadsheet and individually organized for each lap.

The KP data were further processed as shown next by deconvolution of the response to account for the inherent delay in probe response to a change in surface potential as the probe moves from one place to another. That delay causes a corresponding smearing of the measured potential profile with respect to the actual profile as the probe travels at a finite speed over the concrete surface.

As part of the equipment set up on a given test date, the feedback loops parameters in the system responsible for zeroing the KP current for automatic potential measurement were adjusted by the operator to seek a compromise between speed of response and stability. The adjustment was made first for the disk placed at 1 cm over the concrete surface and then after connecting a potential source between the ground of the system and the rebar assembly. The source was made to vary in steps between 0 and 0.3 V, and the response of the automatic zeroing system observed. The speed of response was then gradually increased so that the approximate characteristic time (see below) was on the order of 1 second. The software control system has built in oscillation instability suppression, but it becomes limited for shorter response times than ~1 second; therefore, response speed is set by the operator accordingly. The process was repeated for the 2 cm gap conditions. The acceptable short response time was found to be typically shorter for a 1 cm than for a 2 cm operating gap, indicating that the former lead typically to more stable and faster response functioning than the latter. The sensitivity increase with a larger operating gap reflects the concurrent lower signal-to-noise ratios and greater effect from small imbalances in compensating for the effect of the active shield inherent bias.

The response delay can be characterized by the function $A(t)$, which is the response of the probe to a unit step change in potential at time zero. $A(t)$ can be obtained by direct measurement or represented by a mathematical function with parameters determined by measurements or curve fitting. Assuming linear system behavior, the potential $Em(t)$ measured by the probe at time t from the start of a lap is convoluted with the step response $A(t)$ by:

$$Em(t) = \int_0^t \frac{\partial\, Ea\,(l)}{\partial l} A\,(t-l)\,dl = \frac{\partial Ea}{\partial t} * A \qquad \text{(Eq.2)}$$

where $Ea(t)$ is the actual value of the potential beneath the probe disk at time t, the symbol $*$ is used to express convolution of the two variables per the integration shown, and l is a dummy integration variable. An equivalent, more convenient formulation is given by Goldman [*18*]:

$$Em(t) = \int_0^t Ea\,(l)\,\frac{\partial\,(A\,(t-l))}{\partial t}\,dl = Ea * \frac{\partial A}{\partial t} \qquad \text{(Eq. 3)}$$

where it is assumed that $A(0) = 0$, consistent with the shape observed experimentally.

Calling $FT(f(x))$ the Fourier transform of the function $f(x)$, the following property is known to apply to apply:

$$FT(f1 * f2) = FT(f1) \cdot FT\,(f2) \qquad \text{(Eq. 4)}$$

where · is the multiplier sign, referring to a term-by-term product of the respective Fourier transforms. Hence, referring to Eq. (3) and obtaining $dA(t)/dt$ from the known function $A(t)$, an estimate of $Ea_{\text{recovered}}(t)$ [abbreviated $Ea_r(t)$] of $Ea(t)$ can be recovered from the data by performing:

$$Ea_r(t) = IFT\,\frac{FT(Em(t))}{FT(dA(t)/dt)} \qquad \text{(Eq. 5)}$$

where IFT is the inverse Fourier transform operator and the division sign refers to a term-by-term division of the terms of the functions operated upon. The array of values of $Ea_r(t)$ was then converted into the corresponding $Ea_r(x)$ for each particular lap by reference to the $x(t)$ record obtained for the same lap.

The step function $A(t)$ for the KP sensors was approximated here by

$$A(t) = 1 - e^{-\rho t}\;\frac{sin(\mu t + \Phi\,)}{sin(\Phi)} \qquad \text{(Eq. 6)}$$

where ρ, μ and Φ are characteristic parameters of a damped oscillatory response to a unit step excitation, with ρ as the main damping time constant, μ as representative of the oscillatory response to the step, and with Φ as a delay factor. For values of μ<<ρ the response reduces further to that of simple exponential decay with

$$A(t) = 1 - \exp(t/\tau) \qquad \text{(Eq. 7)}$$

where $\tau = \mu^{-1}$ is the characteristic decay time. In those cases it was found that τ was typically on the order of 1 s. Under those circumstances for each set of laps performed at a given operating probe gap and on a given date, a refined global empirical estimate of the value of τ was obtained by comparing, for selected rows, the graph corresponding to $Ea_r(x)$ when one of the dual probes moved in the N–S direction, with the graph for the other dual probe moving over the same path in the S–N direction. The value of τ was initially taken to be 1 s and then varied until the best overall visual match for the forward and return graphs was obtained; the corresponding optimal value of τ was then used globally for deconvoluting the rest of the peer data for that test date and operating gap. The same values of τ were used for deconvolution of the results from the other special tests on May 19, 2016.

For the purposes of visual map presentation and comparison with the CSE surveys, the deconvoluted KP data from each lap of the basic scans were spatially averaged over 40 cm intervals centered on each of the

grid points other than those at the north and south ends. For those (column 15 for May 19, 2016, columns 1 and 15 for July 27, 2016) an approximation was used by assigning to the point the average of the data for the closest 20 cm. A similar scheme, but with rows twice as long, was used to display the extended length scans performed on July 27, 2016.

Potential maps of both the CSE data and the KP arrays were obtained using contour mapping with an 8-step color-coding scheme, with breakpoints evenly distributed from maximum to minimum in the range of values obtained. To avoid non-informative noise detail all the data were subject to a smoothing procedure whereby the potential at a given point of the grid was blended with a weight factor of 0.25 for the central point potential and 0.75 for the average of the potential at the four points located N, S, E, and W of the central point, with equivalent mirror weighing for edge and corner points. Potential survey summaries of extreme values and range of values were obtained using the smoothed procedure values, to avoid unrepresentative effects from local data noise.

4.2.2.4 Field Test 1 (May 19, 2016) results

4.2.2.4.1 Basic grid tests

Figure 25 shows relative potential maps of the surface of the basic grid obtained using the conventional CSE contact method and two repeat surveys using the dual KP array operating at gaps of 1 cm and 2 cm. A 2.8-m-wide, 5.5-m-long deck surface was surveyed. The color coding identifies the most negative steel potentials in each scan (most active steel with highest likelihood of corrosion) with the reddest hue and the least negative (less likelihood of corrosion) with the bluest. The potential spans obtained in each case are summarized in Table 2. The values of the deconvolution parameters used are listed in Table 3.

Table 2 Summary of Field Test 1 Surface Potential Surveys

Method	E_{min} (V)	E_{max} (V)	Range (V)
Conventional CSE	-0.536	-0.118	0.417
KP Array—1 cm Gap - Scan A	-0.749	-0.209	0.539
KP Array—1 cm Gap - Scan B	-0.727	-0.106	0.622
KP Array—2 cm Gap - Scan A	-0.834	-0.258	0.576
KP Array—2 cm Gap - Scan B	-0.847	-0.295	0.552

Table 3 Deconvolution Parameters for Field Test 1 Tests, Abstracted from Step Response Data

	ρ (s^{-1})	μ (s^{-1})	Φ
T1 cm Gap	1.56	0.09	0.70
2 cm Gap	1.50	0.70	0.47

It is noted that the visual appearance of potential maps can vary significantly depending on the choice of color scheme, the number of color levels used, and the choice of potential value breakpoints used for the transition between colors. In the present case, those parameters were kept as stated earlier with no custom

manipulation in any of the figures. Hence, color assignments of consecutive value intervals (e.g., from red to orange or light blue to light green) and the corresponding boundary lines should not be interpreted as critical indicators of a sharp potential transition. Instead, the maps should be examined for indications of overall trends over relatively large value transitions.

With the above proviso in mind, the conventional CSE survey clearly identified a corroding region on the left center portion of the basic test grid region, with indication of more passive steel on the right side (near the deck lane divider, see Figure 24) and near the south and north ends, especially on the right side.

The KP array surveys using 1 cm and 2 cm gaps successfully identified the same broad features as in the CSE test, including the negative steel region indicative of corrosion on the center left side of the field, and the results were consistent in both A and B repeat tests.

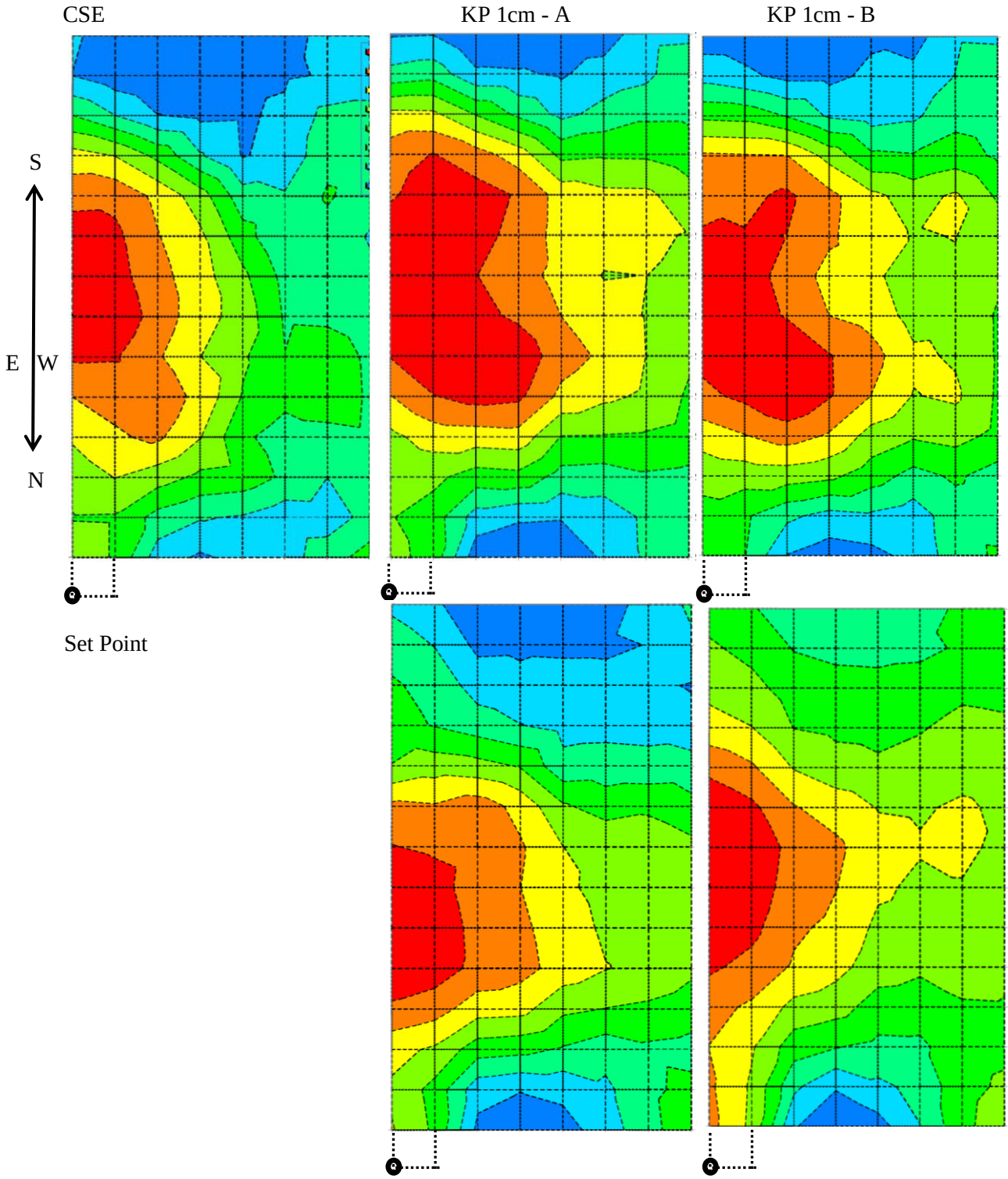

Figure 25: Field Test 1 (May 19, 2016)—potential maps of the basic grid region (0.406 m on center). Top Row: obtained by conventional contact electrode CSE survey (*left*) and with the dual KP array (*center* and *right*, duplicate tests) with a 1 cm operating gap. Bottom Row: Dual KP array potential maps obtained with a 2 cm operating gap. The Set Point (see Figure 24) is at the lower left corner. Painted traffic lane divider (centerline of bridge) runs N–S along the center of the rightmost grid row.

The range of potentials in the KP array tests tended to be about 0.16 V greater than that of the CSE results, and with the color scheme chosen the highlighted corroding region was somewhat broader than that in the CSE map. Nevertheless, the tests demonstrated that the KP array was able to consistently produce the kind of information that would flag high corrosion probability regions in a bridge deck survey, operating in a multiple probe coordinated mode and scanning the region at a speed on the order of 0.3 to 0.6 m per second without the need for prior surface preparation.

4.2.2.4.2 Additional tests for effect of localized surface condition

These tests were of a brief nature and intended primarily to establish whether there was any strong disturbance in the potential readings of the KP probes due to the presence of some common deck surface features. The results presented are as-obtained raw data, with no deconvolution or local integration used to convert the continuous record into a discrete grid point reading. No calibration of one sensor versus the other is implemented either; therefore, only results of relatively large magnitude would be deemed to be relevant. The interpretations in the following are to be regarded as tentative and these issues merit more detailed study in the future.

Paint Line: Figure 26 shows the results of the Run Over Paint Line (ROPL) tests, where laps 1, 3, 5, and 7 denote the potential data for consecutive forward runs over the 120-cm-long scan interval. The dotted line region indicates the position of the ~15-cm-wide lane separating painted line. Within the ~100–150 mV reproducibility raw data interval of consecutive forward laps there were hardly any appreciable systematic effects of the presence of the paint line. A possible exception is a ~20–30 mV potential step in Lap 1 associated with the position of the paint line; however, the step is not apparent in subsequent laps and obscured by the larger lap-to-lap variability band noted above. Overall, the results did not present conclusive evidence of the presence of the paint line having any important effect on the result of the potential readings.

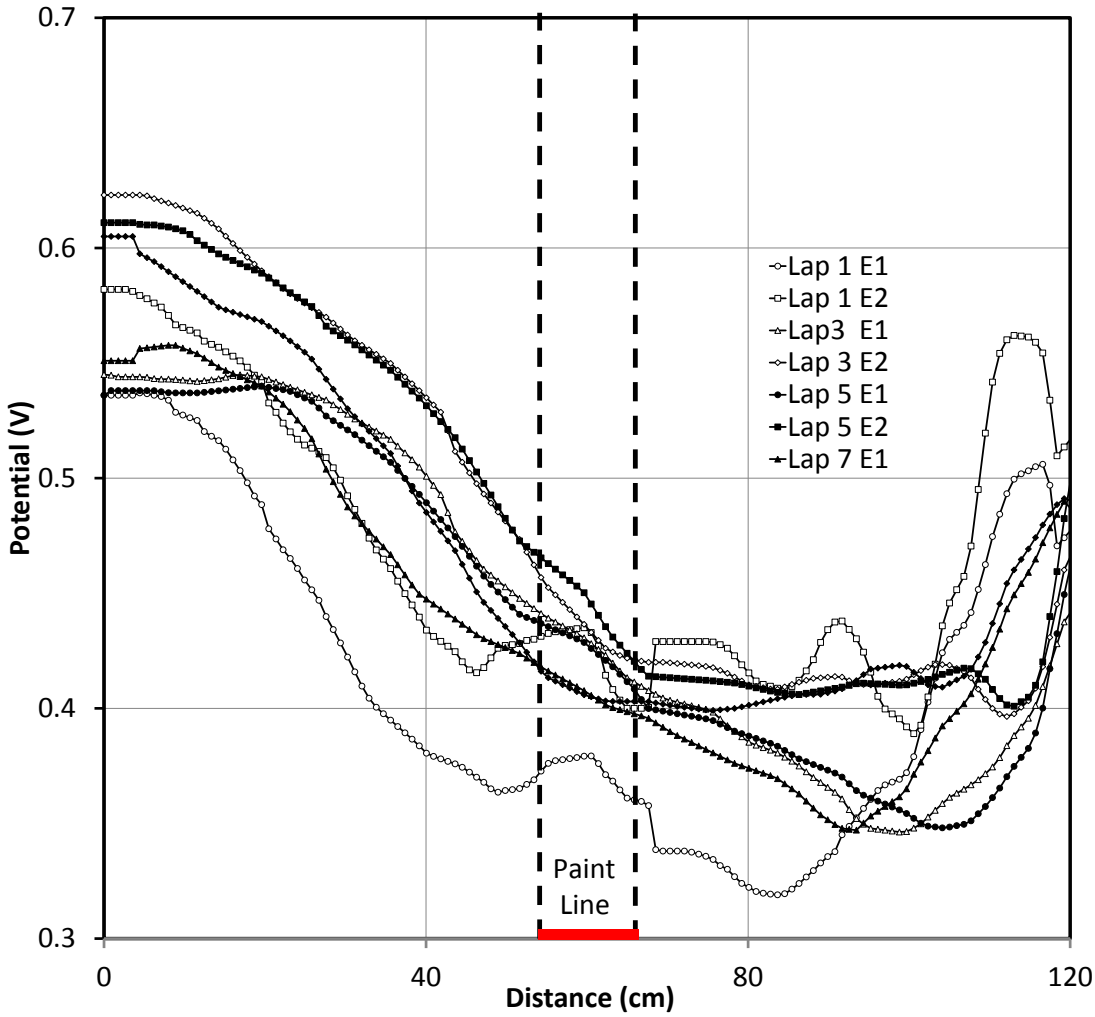

Figure 26: Run Over Paint Line (ROPL) test results.

Wetting: Figure 27 shows the results of the Run Over Water Spots (ROWS) tests, displaying raw scan data as done above. The ROWS tests were done after the ROPL tests and the region scanned overlapped with those.

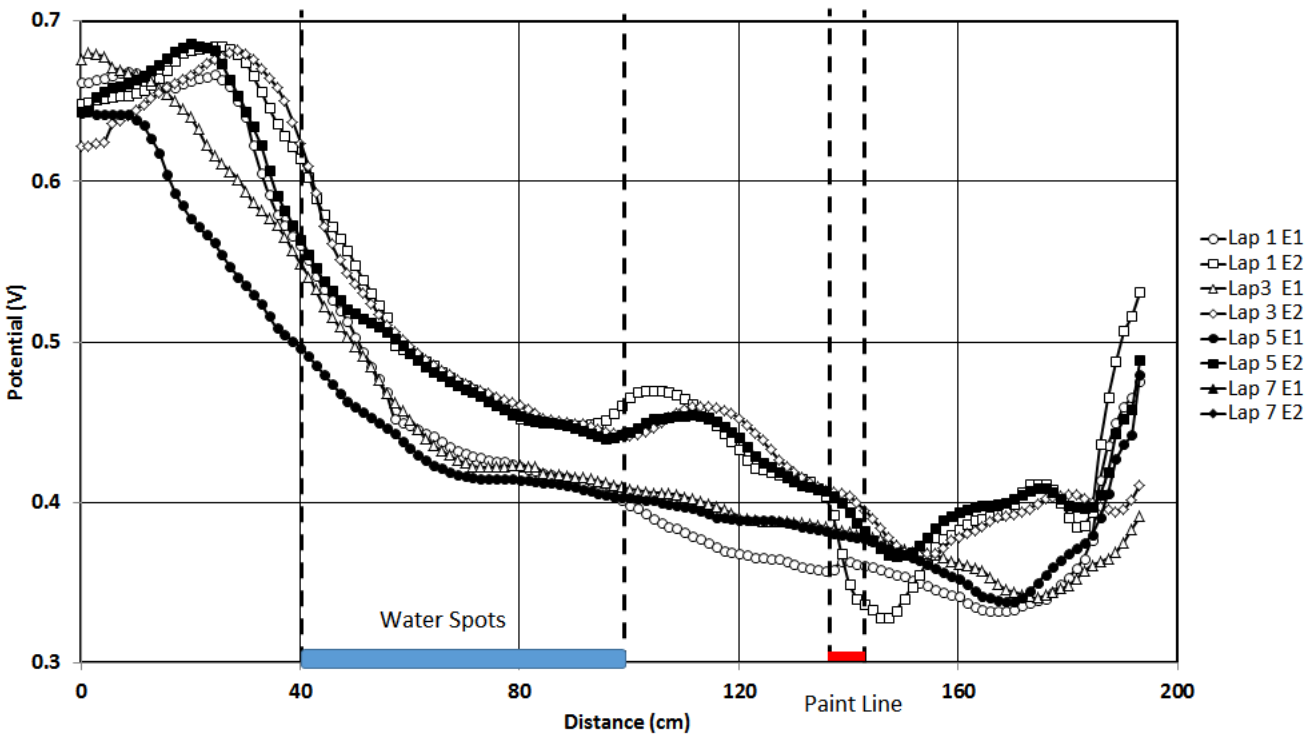

Figure 27: Run Over Paint Line (ROPL) test results.

The traces within the figure by themselves do not indicate a clear effect of local wetting over the potentials recorded for that zone. However, comparison with the ROPL results in Figure 26 (obtained before wetting) suggest that wetting may have caused a local decrease in potential by about 150 mv at the commonly shared position that corresponds to 100 cm in Figure 27. While affected by uncertainty as noted earlier, this finding suggests that KP potential evaluations would be best conducted on a uniformly dry deck surface until further information becomes available on the extent of the error that may be induced by localized wetting.

Motor Oil: Figure 28 shows the results of the Run Over Oil Spots (ROOS) tests, using raw output as for the previous two cases. For clarity the data for both sensors (each of which passed over an oil spot at the same time) are shown separately. The traces obtained during an earlier scan as part of the regular basic grid are shown for comparison as well. The data suggest that there is a moderate potential dip (e.g., on the order of 0.1 V) at the location of the oil spots that was not present in the previous scans. However, at other locations away from the spots there are also non-localized differences of comparable order, which reflect normal variability of results from lap to lap so the association of the dip with the presence of the oil spot is somewhat uncertain. In any case, the effect if present is only of moderate magnitude. This observation, pending confirmation in follow-up investigations, is of interest. There was initially some concern that significant

amounts of tribologic surface potential differences; for example, on the order of tens or hundreds of volts, could be generated, for example, by automobile tires running over spilled oil, and retained for some time due to the insulating effect of the oil. Such random static electricity levels, if present, could greatly affect the sub-volt potential difference patterns sought to be measured during corrosion condition assessment. In the present case, rubbing action during wiping of the surface during preparation of the spots provided an opportunity for that type of event. The absence of severe potential pattern deviation being manifested when the sensors passed over the oil spots offers some degree of assurance that static electricity effects of such extent are not easily created.

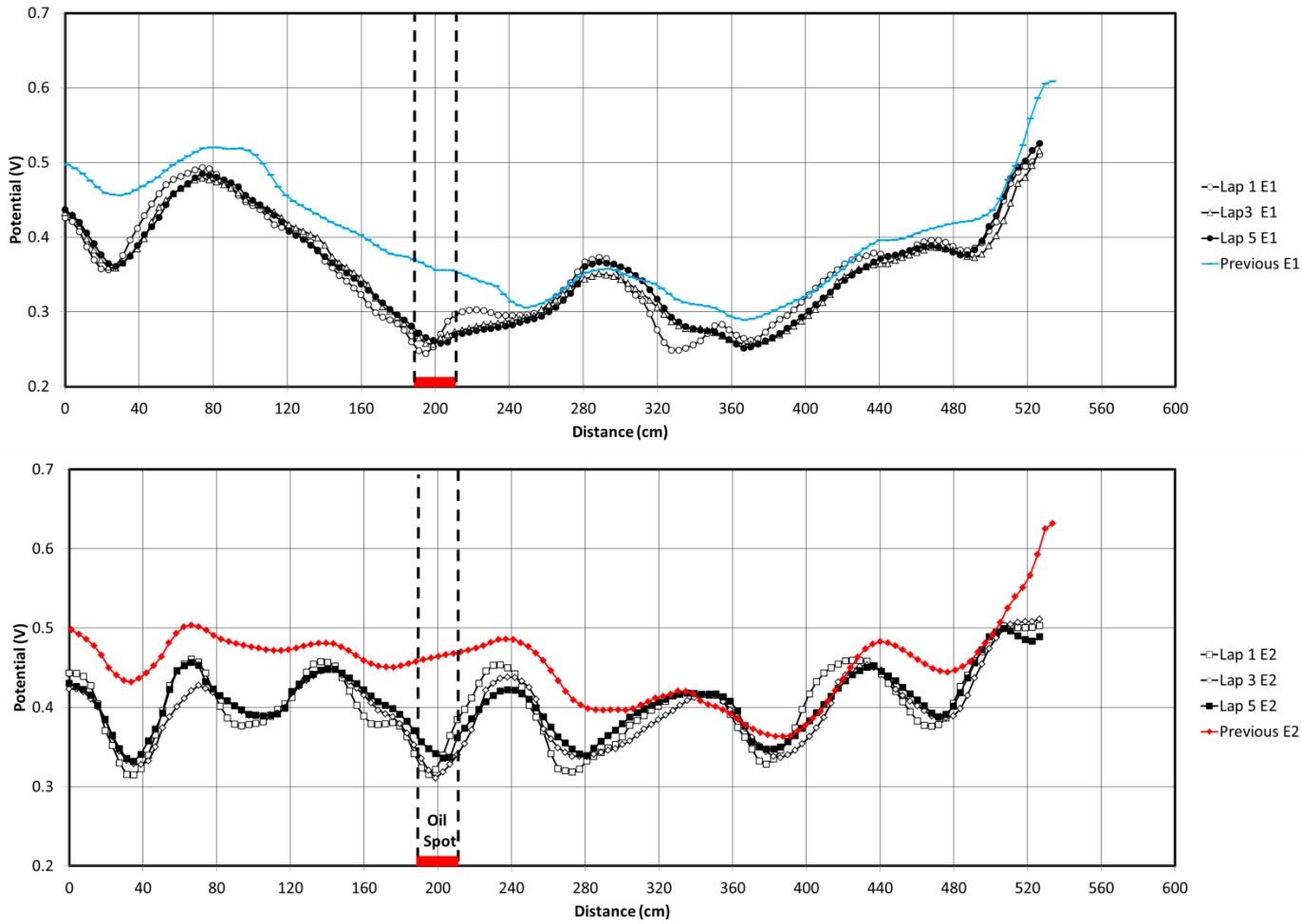

Figure 28: Run Over Oil Spots (ROOS) test results.

4.2.2.5 Field Test 2 (*July 27, 2016*) *results*

4.2.2.5.1 Basic grid tests

Figure 29 shows relative potential maps of the surface of the basic grid obtained using the conventional CSE contact method and two repeat surveys each using the dual KP array at 1 cm and 2 cm operating gaps. In this test date the dual probe scans started at the set point itself so the entire basic 8 by 15 point grid was covered, corresponding to a 2.8-m-wide, 5.7-m-long deck surface. The potential spans obtained in each case and deconvolution parameters used are summarized in Tables 4 and 5.

Table 4 Summary of Field Test 2 Basic Grid Surface Potential Surveys

Method	E_{min} (V)	E_{max} (V)	Range (V)
Conventional CSE	-0.482	-0.108	0.374
KP Array—1 cm Gap - Scan A	-0.652	-0.205	0.447
KP Array—1 cm Gap - Scan B	-0.66	-0.194	0.465
KP Array—2 cm Gap - Scan A	-0.674	-0.16	0.513
KP Array—2 cm Gap - Scan B	-0.724	-0.092	0.633

Table 5 Deconvolution parameters for Field Test 2 Tests, Abstracted From Step Response Data

	ρ (s^{-1})	μ (s^{-1})	Φ
1 cm Gap	2.02	3.17	0.90
2 cm Gap	0.93	0.00	0.52

Keeping in mind the qualifications noted earlier on the graphic nature of the potential maps, the CSE pattern was quite similar to that obtained on May 19, 2016, suggesting that the underlying steel corrosion distribution had not changed markedly during the intervening 2 month period, with a strongly active steel indication on the center of the E side (*left*) and a suggestion of an enlargement of the active steel zone toward the lower left (NE) of the pictured frame. The 1 cm operating gap KP dual array potential pattern reproduced to most of the features seen by the KP in the first test date, as well as similarly identifying the negative potential zone on the E side of the basic grid. The 1 cm KP dual array data also indicated an extension of the active zone to the NE direction, but with much stronger emphasis than that shown in the CSE pattern. The replicate KP 1 cm scan sets (A and B in Figure 29) provided essentially the same results confirming the probe array ability to operate reproducibly.

In this test date the 2 cm operating gap KP dual array potential patterns were affected by an appreciably larger amount of random scatter than that of the 1 cm operating gap tests. As discussed further later on, this occurrence partly reflected the noise sensitivity of the deconvolution output, which for this operating gap and this test date dealt with delay time constants about twice as long as those for the 1 cm gap tests. Nevertheless, the overall potential pattern still identified the presence of a distinctly active region on the center of the E side plus an extension toward the NE corner. The finer fragmentation of the active region into more (red) or less (orange) negative regions displayed in the 2 cm maps is not likely to be very meaningful given the increased uncertainty of results at this operating gap. Keeping that in mind, the replicate tests (A-B) provided results that still reproduced adequately the main pattern features.

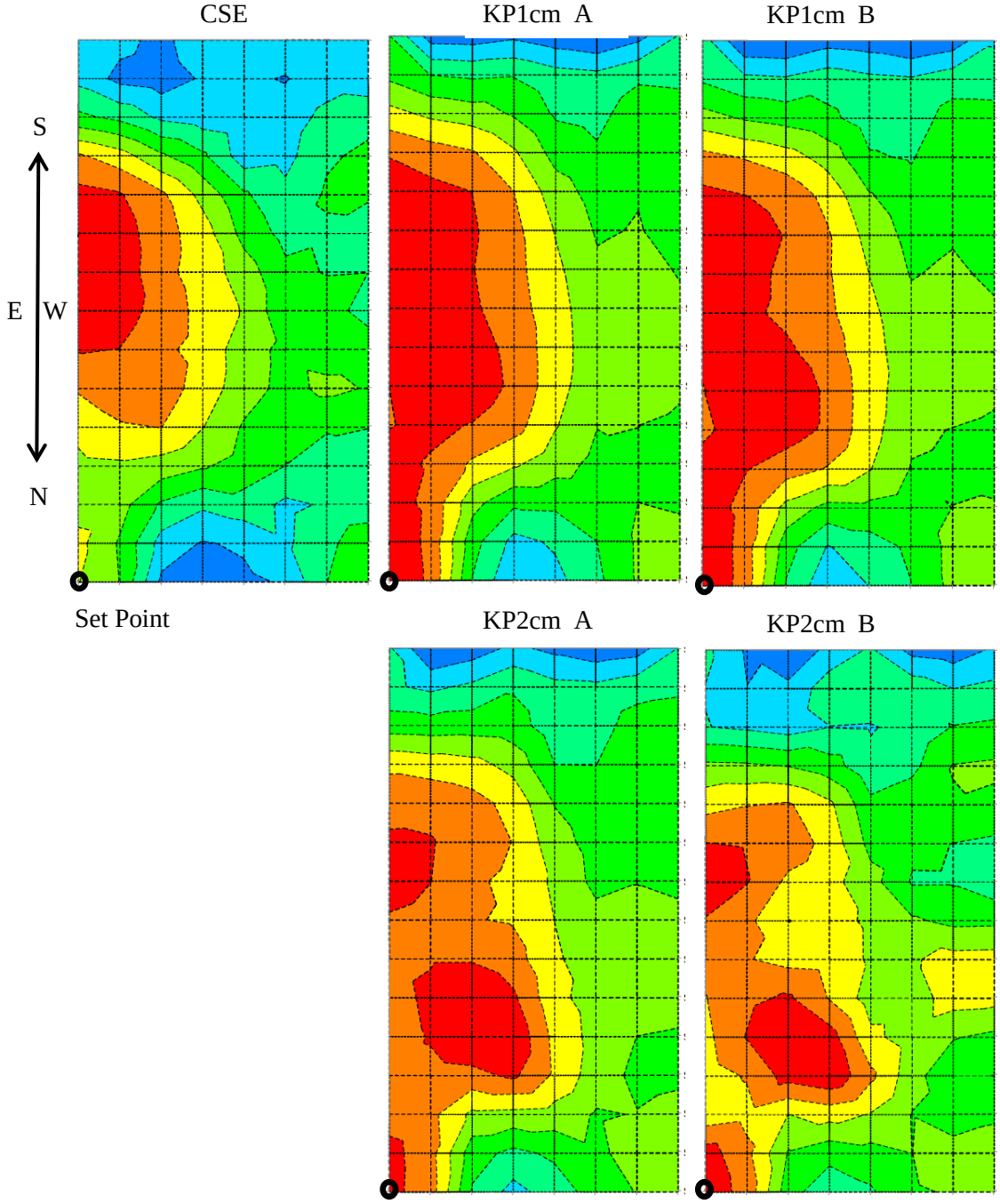

Figure 29: Field Test 2 (July 27, 2016) potential maps of the basic grid region (0.406 m on center). Top Row: obtained by conventional contact electrode CSE survey (*left*) and with the dual KP array (*center* and *right*, duplicate tests) with a 1 cm operating gap. Bottom Row: Dual KP array potential maps obtained with a 2 cm operating gap. The Set Point (see Figure 24) is at the lower left corner. Painted traffic lane divider (centerline of bridge) runs N–S along the center of the rightmost grid row.

4.2.2.5.2 Extended domain tests

Figure 30 shows the 1-cm and 2-cm, operating-gap-extended test results, covering a 2.8-m-wide, 11.4-m-long, long deck surface. As this was a supplemental test, CSE measurements of the added S portion of the surface were perfunctory and covered only the easternmost six grid spaces; therefore, mapping is limited to those for the entire extended map. KP measurements however covered the entire region (with laps running continuously over the entire extended length) and are displayed accordingly. Table 6 summarizes the extremal measurements for each of the tests.

As in the rest of the tests, there was steady state scanning speed (after initial acceleration and final slowdown was on the order of 0.6 m/s), so typical lap times were on the order of 20 seconds each. The extended region included a few spots where the deck surface had shallow blemishes (about 2 cm deep, around 10 cm in diameter) that caused some vibration when the 15 cm diameter wheels passed over. Also, no thorough broom cleaning had been done on that surface, so some minor debris existed. Nevertheless, with the exception of brief excursions when riding over blemishes, potential readings were continuous and noise-free enough to permit processing and deconvolution as in the basic grid region case. It is noted that in one of the 1 cm surveys (B) KP data acquisition was inadvertently stopped ~1 m short of the S end of the last (westernmost) lap. Data for that short segment are blanked out in the corresponding map.

Table 6 Summary of Field Test 2 Extended Grid Surface Potential Surveys

Method	E_{min} (V)	E_{max} (V)	Range (V)
Conventional CSE	-0.482	-0.108	0.374
KP Array—1 cm Gap - Scan A	-0.712	-0.129	0.582
KP Array—1 cm Gap - Scan B	-0.644	-0.121	0.523
KP Array—2 cm Gap - Scan A	-0.707	-0.086	0.62
KP Array—2 cm Gap - Scan B	-0.774	-0.039	0.813

The 1-cm operating-gap-extended CSE map revealed a region of moderate activity on the east side of the center of the newly sampled south portion. That region was clearly apparent also in the same portion of the maps obtained for the dual KP array operating with a 1 cm gap (which, as expected, also reproduced well the strongly active indications obtained earlier for the basic grid side of the scanned deck surface). The 2 cm dual KP array results also flagged the moderately active region in the newly sampled surface, and reproduced as well the features obtained in the earlier sampling of the basic grid portion. As noted earlier for this test date, the 2 cm gap results were again affected by scatter to some extent, but still yielded a meaningful broad picture of the potential pattern of the extended deck surface sampled.

The scatter present in the 2 cm tests was accompanied also by greater broadening of the range of potential values in the same tests (on average ~0.55 V compared with 0.37 V in the CSE tests). This broadening reflects some degree of instability in the deconvolution process, partly due to the presence of a relatively low value of ρ for the 2 cm parameters (Table 5). That parameter is inversely proportional to the equivalent time constant of the step response, indicative that for the instrumentation settings used in the July 27, 2016, tests the operator-chosen response of the system with operating gap of 2 cm was relatively slow. Due to the factors mentioned in a previous section, the latitude in choice of system settings becomes greater for the 2 cm operation, with consequently increased possibility of added scatter in those measurements.

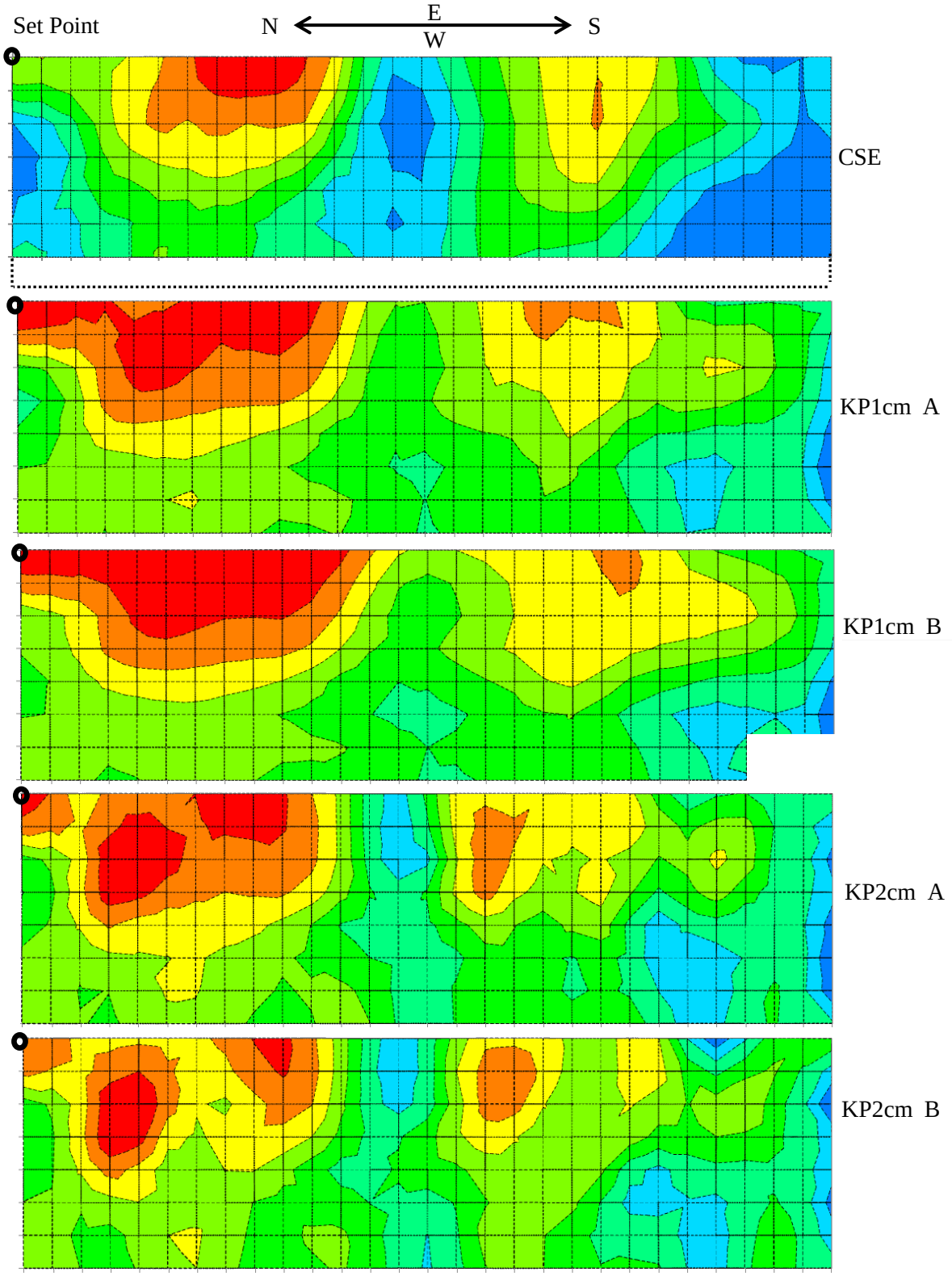

Figure 30: Field Test 2 (July 27, 2016) potential maps of the extended grid region (0.406 m on center). Top: obtained by conventional contact electrode CSE survey. Rest: obtained with the dual KP array, with 1 cm and 2 cm operating gaps replicated (A-B) in each case. Set Point per Figure 24 is indicated. Painted traffic lane divider (centerline of bridge) runs N–S along the center of the westernmost grid row.

Based on the above and on the observed combination of quite stable results for May 19, 2016, but greater scatter in July 27, 2016, a 2 cm operating gap appeared to approach the upper practical value for the prototype as constructed. However, there is no theoretical limit for the disk-to-concrete surface operating gap, and wider gaps should be feasible given subsequent design improvement as discussed next.

4.2.2.6 Overall comments, field test results, and mode enhancement

The field tests provided, as the main outcome of the project, a demonstration of the practical feasibility of the concept of using a rapidly scanning contactless surface probe to conduct potential mapping of a highway bridge surface for corrosion detection. The KP maps successfully replicated the features obtained with the conventional contact electrode mapping procedure, but at a much faster rate and without need of preparation of the surface or waiting time for stabilization. The field tests also demonstrated the practical feasibility of multiple probes operating together and in synchronized fashion to scan simultaneously parallel portions of a lane in a bridge deck. While the present work scope was limited to two coordinated probes, the signal processing methodology developed here could be easily expanded, with ordinary consumer's electronics, to six or eight sensor arrays as in Figure 5, sufficient to cover the width of an entire traffic lane. The project demonstrated also, per the initial scope of work, that the KP array operated successfully at hand-drawn sensor speeds of about 2 km/h. Even at that moderate pace potential surveys in many instances could be conducted in very short times, assuming that a rebar contact has been prepared beforehand. For example, an entire traffic lane along a moderate length highway bridge (e.g., 0.3 km long) could be surveyed in about 10 minutes. That fast operation compared with the burden imposed by traditional techniques would greatly lessen the need for traffic control. As discussed in the Stages 1 and findings, there are promising prospects for optimization in operating speeds, perhaps by an order of magnitude or greater than those used in the field tests, with consequent potential for further marked lessening of the traffic disruption associated with the survey.

The KP field test output was consistently stable and with relatively little scatter for the system operating with a 1 cm operating gap. Performance with the 2 cm gap gave mixed results, with quite stable measurements in the May 19, 2016, tests but with significantly greater scatter in the July 27, 2016, tests. The latter scatter is perhaps attributable to suboptimal setup of the step response of the probes at the time. Nevertheless, while approaching the practical limit for the present prototype, the 2 cm scan results still provided useful results, even in the second test data. In broader applications the operating gap should be as wide as possible to avoid potential physical damage or surface contamination of the disk in case of extreme deck surface roughness or blemishes. Hence, future development of production units should seek to improve the design to extend as much as practical the operating gap capabilities of the system. Promising optimization development avenues to that end include the use of somewhat larger diameter disks and larger shields, so that the relative effect of extraneous signals is diminished, use of larger vibration amplitudes used to improve signal-to-noise ratio, and exploration of more sophisticated data deconvolution methods create a more robust recover potential profile than the one used here.

All measurements demonstrated in this report were conducted in the Absolute mode (Section 3), which requires a master wired connection to some point of the rebar assembly in the bridge deck to be assessed. Consecutive bridge spans, if to be mapped in the same scan, should have electric continuity of rebar implemented and verified from each span to the next. For efficient use of the KP Absolute mode, the master

connection would best be made in a prior visit to the structure and set up as a weather resistant connector; for example, a stainless steel stud, emerging as a convenient point at one end of the bridge, such as next to a guardrail or similar accessible feature. The trailing wire would then be paid off from a reel as the KP assembly progresses along the traffic lane to be assessed; the reel would be wound up at the end of the scan.

The alternative Differential mode (Section 3) would provide only relative surface potentials (although it could be supplemented by only one or a few punctual conventional potential measurements, thus yielding an absolute potential calibration), but would obviate the need for a trailing wire. Methodology for obtaining differential potential maps without rebar connection has been demonstrated by other investigators for arrays of surface contacting electrodes, for example as in Reichling and Raupach [*19*]. In this project a Differential mode implementation has been developed (limited mainly to the conceptual level) for an array of contactless KP probes by means of the addition of one auxiliary contacting electrode. The operational scheme is shown in Figure 31.

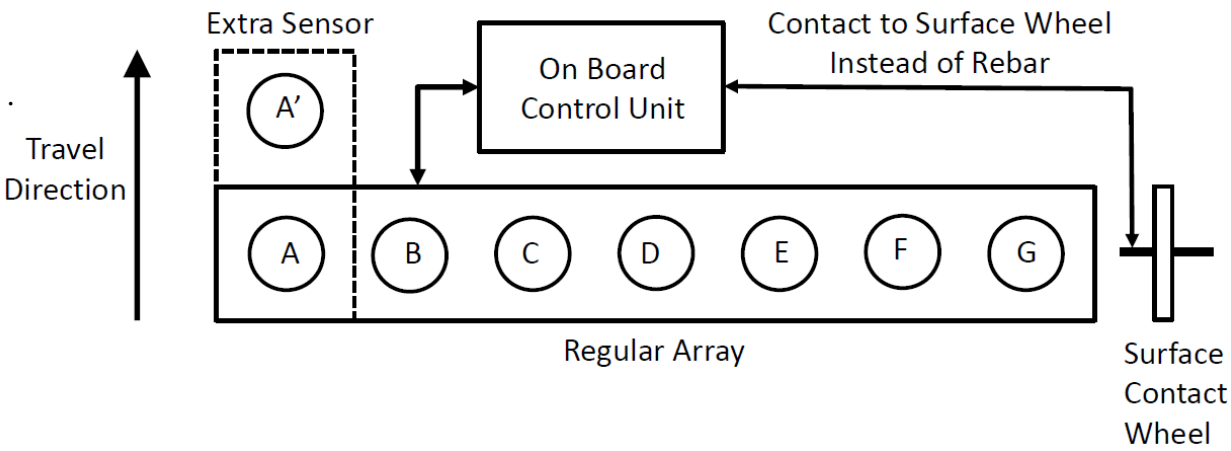

Figure 31: Conceptual Differential mode scheme, top view.

A regular KP array consisting of probes A to G is mounted on a trailer that moves and acquires surface potential data on a given traffic lane in the indicated travel (longitudinal) direction. A deck surface contact metallic wheel with a rim made of a soft conducting material (either conductive rubber or a lightly moist artificial sponge strip) provides an auxiliary moving deck surface contact point. That contact point acts as an auxiliary electrode that adds to the potential readings an unknown potential value relative to the rebar mat, but that has a contact impedance low enough to allow for low noise potential readings of sensors A to G. Thus, at any given position in the longitudinal direction the array provides the actual differential transversal potential profile E_A - E_X, where E_A is the potential measured by sensor A, and E_X is that measured by any of the remaining B to G sensors. However, there would not be a reliable indication of the potential profile in the longitudinal direction as the wheel-added potential is unknown and could vary appreciably as the wheel rolls over different points of the deck surface. That difficulty is removed in the present scheme by the use of an additional KP sensor A', as shown in Figure 31. At any given longitudinal position of the trailer, the potential difference E_A (and hence $E_{A'}$ - E_A) is obtained and recorded simultaneously with the other potentials. Thus, a potential measurement link is provided along the travel direction so that when A moves into the position formerly occupied by A' the new transversal profile can be referred reliably to the one in the previous longitudinal position.

Feasibility trial tests were conducted with a lightly moistened artificial sponge that formed an ~3 cm wide strip on the rim of an ~15-cm-diameter metallic wheel, with the dual KP array set to a 1 cm operating gap and standing on the test yard test slab used for the Stage 1 experiments. The system showed appreciably stable potential readings in each probe (e.g., short-term random variations comparable to those observed in the Absolute mode), confirming that the auxiliary electrode contact had low enough impedance for adequate KP probe operation. Test of the entire operation with the dual KP array in motion are to be conducted in future follow-up investigations. An important issue to be examined at that time is the possible importance of small but systematic cumulative errors in the value of $E_{A'} - E_A$ as the array progresses longitudinally, which would be manifested as a false longitudinal ramp in the potential values along the longitudinal direction. Approaches for compensation of those cumulative effects may need to be developed, for example, by means of additional readings with a second auxiliary contacting electrode placed at a known distance from the first.

Based on feedback from reviewers of this project, it is anticipated that implementation of the Differential mode could significantly improve the likelihood of commercialization of the KP method. Potential users may find quite attractive the substantial time and complication savings from avoiding the need for setting up a rebar connection, even at the expense of some loss of information from absolute potential measurements. Hence, future development effort toward implementing the Differential mode including field demonstrations should be given high priority.

5. PLANS FOR PRODUCT IMPLEMENTATION

Availability of contactless probe systems could dramatically expand the development and updating of corrosion condition information on much of the national bridge deck inventory in deicing salt and marine regimes. Operations that in the past required extended lane closures and costly labor contracts could now be conducted with minimal traffic disruption and at a fraction of the cost. Hence, corrosion diagnostics could be conducted routinely and frequently; for example, concurrent with regularly scheduled periodic bridge inspections. Frequent evaluations have the added benefit of aiding to reveal evolving features that would be missed in a single time, snapshot survey. The resulting aggregate data could then be an integral feature of the bridge maintenance record, providing transportation agencies with an important added tool in assessing the need for remedial action and for forecasting future resource demands.

Importantly, the contactless probe systems would also enhance the collective safety of a state transportation system by providing early warning of corrosion damage. That damage would otherwise have remained undetected, if evaluation had to wait until resources became available for a conventional potential survey.

The work in the project has shown that materials, circuitry components, and mechanical parts needed to construct this type of equipment in future commercial units are commonly available and readily adaptable from present day technology. Durability limitations, maintenance needs, and unit cost are not anticipated to be unusually different from those of other mobile highway diagnostic methods.

The University of South Florida Technology Transfer Office—Patents & Licensing, together with the Principal Investigator initiated communications with two possible industrial partners for commercialization of the project product, which involves aspects of USF#11B142 utility patent application 13/905,761 "Systems and Methods for Contactless Assessment of Reinforced Concrete," filed May 30, 2013. The outcome of those communications is pending. Further product development could take place with sources such as funding from investors, other government agency and development programs, and university cooperative efforts, if appropriate.

It is expected that developed systems will become commonly available for purchase or rental by state transportation agencies, port authorities, or other institutional entities that become the principal service customer base and potential operators of the systems. Feedback from project reviewers suggests that this mode of implementation may be the most economically attractive for state transportation agencies, especially if a sizable bridge inventory is to be surveyed. Alternatively and contingent on pricing, the units could be used and operated by consulting firms that would provide an integrated measurement, interpretation, and reporting service to the institutional users. In either alternative, interpretation of the data can readily take place following already established practice for potential surveys and with existing expertise from state transportation agencies or their consultants.

Furthermore, contact has been established with the FHWA Long Term Bridge Performance Program (LTBP) to discuss possible integration of this potential mapping method in the Robotic Assisted Bridge Inspection Tool (RABIT™ [*20*]). That unit is a wirelessly operated robotic unit that incorporates several bridge deck assessment sensors for which a contactless KP, especially in the Differential mode, may be a powerful addition for corrosion detection. Similar cooperation is being sought with remaining or follow-up tasks conducted under the SHRP 2 field validation testing of NDT technologies in concrete bridges. Whenever appropriate, those activities will be coordinated with the collaborative tests that were conducted with Florida DOT cooperation at the Sunshine Skyway Bridge.

Additionally, dissemination of the findings of this project and related publications supporting the operating concept has been presented as follows:

- Paper by Walsh and Sagüés illustrating the application of KP for potential surveys and corrosion measurements in concrete was published at an international conference on ageing of structures in Delft, the Netherlands [*21*].

- Poster titled "Contactless Electrode for Fast Survey of Concrete Reinforcement Corrosion," by Sagüés and Emmenegger was displayed at the TRB 94th Annual Meeting, January 11–15, 2015, Washington, D.C., Session 296: TRB's NCHRP IDEA Program: Sponsoring Innovation in Highway Transportation.

- Poster titled "Contactless Electrode for Fast Survey of Concrete Reinforcement Corrosion" by Emmenegger [*22*] was presented at the Student Poster Session of Corrosion/2015 Annual Meeting of NACE International, March 15–19 2015, Dallas, Texas. The poster was awarded the Harvey Herro Applied Corrosion Technology Best Student Poster prize, 2nd place.

- Presentation by Sagüés and Emmenegger, "Mobile Contactless Electrode for Fast Survey of Concrete Reinforcement Corrosion," NACE–ACI Concrete Service Life Extension Conference, May 23–25, 2016, Orlando, Florida.

- Paper by Sagüés et al. [*23*] illustrating application of KP for measurements in CLSM cementitious fill and soil, International IEEE Sensors 2016 conference proceedings (2016).

6. CONCLUSIONS AND ACHIEVEMENTS

1. An initial conceptual Kelvin Probe (KP) for contactless steel potential survey of reinforced concrete was scaled up dimensionally in both disk diameter (to 10 cm), disk-to-concrete surface gap (to as much as ~2 cm), and in an electromagnetic driving unit (to a commercially available vibrator operation) in a rugged configuration suitable for an actual road surface

2. Laboratory tests with the scaled-up probe showed that corrections for operating gap changes may be conducted by appropriate calibration. Hence, precise real-time gap control beyond that achievable by appropriately selected wheel base dimensions was not found to be necessary.

3. Test runs conducted with a single probe prototype on laboratory specimens and on an outdoor large size slab demonstrated the ability to acquire potential maps. The contactless probe potential maps on the outdoor slab successfully identified the anodic (corroding) spot in the slab and provided information in good graphic agreement with that obtained by conventional CSE electrode surveys. The tests also illustrated how calibration for absolute potential measurements can be conducted.

4. Analysis of single probe operation parameters for measurements in moving vehicles was conducted, indicating good potential for readings at practical speeds. An alternative mode was proposed for future examination.
5. The single KP was duplicated and the two units integrated as a dual KP array capable of synchronized operation. The dual probe array was built on a robust wheeled platform. The dual KP array includes digital signal processing and control operating from a laptop computer and off-the-shelf data acquisition boards, active shields that provide compensation for operating gap variations, and adjustments for optimizing probe response speed with system stability. A specialized data deconvolution procedure was developed and successfully deployed to allow for better interpretation of results obtained with the probe array in motion.
6. Probe operation was demonstrated by two field test series conducted at a bridge deck exposed to marine service conditions, part of the former west access road of the old Sunshine Skyway Bridge in Tampa Bay, Florida. Both tests series included operation of the dual KP array with operating gaps of 1 cm and 2 cm, and contrasting the results with those from a potential survey of the same deck portion with a conventional CSE. Limited tests also evaluated the possible influence of deck surface conditions including painted lane dividers, wetting, and motor oil spots, on the readings by the dual KP array.

7. The field tests provided, as the main outcome of the project, a demonstration of the practical feasibility of the concept of using a rapidly scanning contactless surface probe to conduct potential mapping of a highway bridge surface for corrosion detection.
8. The contactless KP maps successfully replicated the features obtained with the conventional contact electrode mapping procedure, but at a much faster rate and without the need for preparation of the surface or wait for stabilization. Result sensitivity to deck surface condition appears to be moderate. The field tests also demonstrated the practical feasibility of multiple probes operating together and in synchronized fashion to scan parallel portions of a lane in a bridge deck simultaneously.
9. The signal processing methodology developed here could be easily expanded, with ordinary consumer's electronics, to a multiple sensor array sufficient to cover the width of an entire traffic lane.
10. Prototype probe operation was best when operating at a 1 cm operating gap. Operation at a 2 cm gap still provided useful results, but increasing scatter indicated that 2 cm is near the upper limit of practical operation at the present state of prototype development. Wider operating gaps are expected to be feasible however given subsequent development.
11. A conceptual approach for Differential probe operation without need for a trailing wire for rebar contact was presented for future development.
12. Availability of contactless probe systems could dramatically expand the development and updating of corrosion condition information on much of the national bridge deck inventory in deicing salt and marine regimes. Operations that in the past required extended lane closures and costly labor contracts could now be conducted with minimal traffic disruption and at fractional cost.
13. Planning for product implementation included contacting potential future potential partners as well as agencies engaged in bridge performance and robotic assessment methods for bridge deck assessment. Work in progress in this project was disseminated at various technical venues.

7 INVESTIGATORS PROFILE

The principal investigator is Dr. Alberto Sagüés, P.E. FNACE. Dr. Sagüés is Distinguished University Professor at the Department of Civil and Environmental Engineering of the University of South Florida (USF). He has a Ph.D. in Metallurgy from Case Western Reserve University and extensive experience in the area of assessment, control, and forecasting of corrosion of steel in concrete, much of it for the Florida Department of Transportation and federal agencies. He has more than 200 technical publications in that area and other materials science, engineering, and instrumentation issues. In addition, he has three patents in corrosion control and has recently filed documentation toward a provisional patent application for the application of a Kelvin Probe for corrosion assessment of steel in concrete, based on the trial experiments described earlier and that have been published in Sagüés and Walsh [*11*]. He personally designed and constructed much of the instrumentation used for that project.

Mr. Leonidas Emmenegger received his M.S. at the University of South Florida with a thesis on developing the initial prototype and software control for this investigation. Mr. Emmenegger has participated in technical presentations at national and international meetings, including receiving a best poster award by NACE International.

8. REFERENCES

[1] Lee, S.K., "Current State of Bridge Deterioration in the U.S.—part 1," *Materials Performance*, Vol.51, No. 1, pp. 62–67, 2012.

[2] Lee, S.K., "Current State of Bridge Deterioration in the U.S.—part 2," *Materials Performance*, Vol.51, No. 2, pp. 40–45, 2012.

[3] Hema, J., W. Spencer Guthrie, and F. Fonseca, *Concrete Bridge Deck Condition Assessment and Improvement Strategies*, Report UT-04-16 to Utah Department of Transportation, Brigham Young University, Provo, 2004.

[4] ASTM C876-09, Standard Test Method for Half-Cell Potentials of Uncoated Reinforcing Steel in Concrete, West Conshohocken, Pa., 2009.

[5] Elsener, B., C. Andrade, J. Gulikers, R. Polder, and M. Raupach, "Half-Cell Potential Measurements—Potential Mapping on Reinforced Concrete Structures," *Materials and Structures* Vol. 36, pp. 461-471, 2003.

[6] Schiegg, Y., M. Buchler, and M. Brem, "Potential Mapping Technique for the Detection of Corrosion in Reinforced Concrete Structures: Investigation of Parameters Influencing the Measurement and Determination of the Reliability of the Method," *Materials and Corrosion*, Vol. 60, pp. 79–86, 2009.

[7] Myrdal, R., "Phenomena that Disturb the Measurement of Potentials in Concrete," Corrosion/96, paper no. 339, NACE International, Houston, Tex., 1996.

[8] Myrdal, R., "Potential Gradients in Concrete Caused by Charge Separations in a Complex Electrolyte," Corrosion/97, paper no. 278, NACE International, Houston, Tex., 1997.

[9] Angst, U., O. Vennesland, and R. Myrdal, "Diffusion Potentials as Source of Error in Electrochemical Measurements in Concrete," *Materials and Structures*, Vol. 42, pp. 365–375, 2009.

[10] Broomfield, J.P., P.E. Langford, and A.J. Ewins, "The Use of Potential Wheel to Survey Reinforced Concrete Structures, Corrosion Rates of Steel in Concrete," ASTM STP 1065, N.S. Berke, V., Chaker, D. Whiting, eds., American Society for Testing and Materials, Philadelphia, Pa., pp. 157–173, 1990.

[11] Sagüés. A. and M. Walsh, "Kelvin Probe Electrode for Contactless Potential Measurement on Concrete—Properties and Corrosion Profiling Application," *Corrosion Science*, Vol. 56, pp 26–35, 2012.

[12] Klein, U., W. Vollmann, and P.J. Abatti, "Contact Potential Differences Measurement: Short History and Experimental Setup for Classroom Demonstration," *IEEE Transactions on Education*, Vol. 46, pp. 338–344, 2003.

[13] Stratmann, M. and H. Strechel, "On the Atmospheric Corrosion of Metals Which Are Covered with Thin Electrolyte Layers—I. Verification of the Experimental Technique," *Corrosion Science*, Vol. 30, pp. 681–696,

1990.

[14] Yang, C., et al., “Inspecting Wafers Using a Potential Difference Imaging Sensor Method,” *MICRO Magazine*, Vol. 25, No.1, 2005.

[15] Emmenegger, L.P., “Kelvin Probe Electrode for Field Detection of Corrosion of Steel in Concrete,” Honors Thesis, University of South Florida, Tampa, Fla., 2014.

[16] Hibbeler, R.C., *Mechanics of Materials*. 8th ed., Prentice–Hall, Boston, Mass., 2011.

[17] Boyd, S.R. and P.D. Krauss, *Highway Concrete Technology Development and Testing: Volume V—Field Evaluation of Strategic Highway Research Program 2* (*SHRP 2*) *C-206 Test Sites* (*Bridge Deck Overlays*), FHWA-RD-02-086, FHWA, Washington, D.C., Aug. 2006.

[18] Goldman, S., *Transformation Calculus and Electrical Transients*, Prentice–Hall, Englewood Cliffs, N.J., 1955.

[19] Reichling, K. and M. Raupach, “Method to Determine Electrochemical Potential Gradients Without Reinforcement Connection in Concrete Structures,” *Cement & Concrete Composites*, Vol. 47, pp. 3–8, 2014.

[20] Lane, S., H. Ghasemi, R. Zobel, and T. Saad, “Long-Term Bridge Performance (LTBP) Program,” presentation at the AAASHTO SCOBS Meeting, Portland, Ore., June 19–20, 2003.

[21] Walsh, M.T. and A.A. Sagüés, “Novel Kelvin Probe electrode for non-intrusive corrosion rate evaluation of steel in aged concrete structures,” in *Proceedings of the 1st International Conference on Ageing of Materials & Structures*, K. van Breugel and E.A.B. Koenders, Eds., Delft University of Technology, Delft, the Netherlands, pp. 569–575, 2014

[21] Emmenegger, L.P., ‘Contactless Electrode for Fast Survey of Concrete Reinforcement Corrosion,” Poster session presented at the NACE International Student Poster Session Corrosion 2015, Houston, Tex., Mar. 2015.

[23] Sagüés, A.A., L.P. Emmenegger, E.A. Paz Velásquez, and W.C. Ruth, “Macroscopic Kelvin Probe for Contactless Corrosion Assessment of Structures Buried in Soil,” *Proceedings, IEEE Sensors 2016*, pp.415–417, IEEE, 2016.